Fabrication of monodispersed spherical thermosensitive gels and their dynamic behavior in aqueous polymeric solutions with temperature gradient

DISSERTATION

Fabrication of monodispersed spherical thermosensitive gels and their dynamic behavior in aqueous polymeric solutions with temperature gradient

Graduate School of Natural Science and Technology
Kanazawa University

Division of Mechanical Science and Engineering

Student ID Number : 1624032018
Name : Raden Rinova Sisworo
Chief Supervisor : Professor Yukio TADA
Date of Submission : 2020.6.26

Abstract

This research studied about fabrication technique of monodispersed spherical thermosensitive gels, specifically factors affecting diameter size of the resulted NIPA gels. The research also investigated swelling and shrinking phenomena of the NIPA gels at various diameters in a constant temperature fields and clarifies the dynamic behavior of the NIPA gels at various diameters inside an upper heating system of a rectangular cavity containing water and polymeric solution. In addition, this work also reviewed factors affecting convective heat transfer inside a fluid-filled rectangular cavity including effect of partially active wall, presence of magnetic fields, application of nanoparticle fluid, and functional particles.

NIPA gels were generated by the cross-linked polymerization of the monomer (NIPA) and N, N'-methylenebisacrylamide (BIS) as cross linker with the aid of Dodecyl dimethyl benzyl ammonium bromide (DDBAB), Tetramethylethylenediamine (TEMED), Ammonium persulfate (APS), and deionized water. The apparatus to fabricate thermosensitive gels including the microfluidic device containing the co two-phased flows were designed and installed. Sizes of the resulted NIPA gels inside the microfluidic device were measured by using MatLab codes for image processing. Apparatus to observe swelling and shrinking phenomena, as well as the apparatus to investigate dynamic behavior of the gels inside the upper heating rectangular cavity were designed and set according to their functions.

The results showed that in fabricating the NIPA gels, continuous-phase flow rate and its kinematic viscosities were the most influential variables in determining the size of monodispersed thermosensitive gels. For the both kinematic viscosities, as continuous-phase flow rate was increasing, diameters of the resulted gels decreased. Higher viscosity of the continuous-phase flow generated smaller diameter of the NIPA gels.

In addition, the NIPA gels showed a swelling state when submerged in a low-temperature solution and exhibited a shrinking state when submerged in a high-temperature solution: demonstrated a negative thermal expansion. For water solution, drastically volume change of the gels occurred at temperature between 25 and 30°C. Whereas, for the PAANa solution, slightly decreased of volume change occurred in the entire ranges as temperature of the solution increased. Furthermore, the NIPA gels

showed vertically repetitive movements for a certain duration of time inside the rectangular cavity of an upper heating system. In a low-temperature solution, the buoyancy force acting on the gel particles exceeded the gravitational force, the size of the gels increased and their densities were lower than that of the solution, then the gels ascended. At higher temperatures, the gels shrank because the gravitational force outweighed the buoyancy force, the gels' densities were higher than that of the solution causing the gels to descend. The gels with a larger diameter tended to have longer durations of vertical movements within the aqueous polymeric solution than the smaller-sized gels and the equilibrium conditions were quickly achieved by the smaller gels.

Keywords: convective heat transfer, thermosensitive gels; polymeric aqueous solution; swelling and shrinking behavior; buoyancy force; gravitational force; vertical repetitive movements

Table of Content

List of Figures

Chapter 1

Introduction

1.1 Background

In engineering perspectives, synergy amongst various fields of study and good collaboration of a team members to support research outcomes is very important. Collaborative research conducted by a number of researchers can increase quality of the outcomes, besides, it can support further cooperation for future goals in terms of academic, healthy, and peace. In this millennium era, competition in some research projects and research products is exist all time in every part of the globe. Competition can drive innovation and increase human welfares but also can damage the research itself if not well organized.

Recently, due to increasing of energy consumption, global environmental problem, such as global warming and desertification and depletion of energy resource occurs. Therefore, utilization of unusable energy and improvement of efficiency of energy device. These techniques contribute the reduction of greenhouse gasses. Improvement of efficiency of energy device are important issue. In order to improve the efficiency of energy device, development of heat transfer enhancement techniques is key technology. The technique of heat transfer enhancement is classified into active method and passive method. The active method has an advantage of high controllability of heat transfer. On the other hand, passive method has an advantage of low external power and no additional devise. As typical passive method, we consider the natural convection heat transfer system. For upper heating system, heat transfer rate is small due to no convection since temperature stratification layer is formed. To improve this inconvenience, addition of

thermo-sensitive particles has been proposed in this study. By using thermo-sensitive gels with negative thermal expansion, convection is generated. Then, heat transfer enhancement without external power will be realized. In this study, fabrication of monodispersed spherical thermosensitive gels and their dynamic behavior in aqueous polymeric solutions with temperature gradient have been studied.

This research studies about generation of monodispersed thermosensitive gels in micro fluidic device and observation of their shrinking and swelling behaviors inside a rectangular cavity filled with water and polymeric aqueous solutions of an upper heating system (lower cooling system). This research is a combination of some mechanical engineering's field of studies including: fluid-flows inside a duct, two phased-flow fluids, polymer-gel material, and heat transfer and control which all synergize as an integrated system.

In general, the thermosensitive gel is classified in a sub class of polymer materials and is also considered as part of smart hydrogels which are directly responding to their external stimuli changes such as temperature, pH, UV/visible light, ion, and solvent compositions [1-3]. Thermosensitive gel can be constructed by physical or chemical crosslinking and is a unique class of polymer materials that can preserve particular amount of water while sustaining their frame [4]. Crosslinking degree in a polymer material plays important roles to strengthen elastic modulus of it and to improve mechanical strength of its network structures. Crosslinking degree of the polymer gel could affect mechanical behavior of the gel when interacting with variation temperatures of the medium and concentrations of polymeric solutions. Thermo-sensitive gels can have either sol-phase or gel-phase condition depends on the temperature of its circumstances. Sol phase is considered as a flowing fluid state meanwhile a gel-phase relates to a rigid non-fluid state while preserving their shape or physical structure. Typically, this sol-gel

conditions can be achieved only by thermal stimulus. Especially for biomedical applications, the condition is suitable for in situ hydrogel formation near humans' body temperature without requiring additional chemical initiators [5]. Furthermore, thermosensitive gel also may have either lower critical solution temperature (LCST) or upper critical solution temperature (UCST) or a combination of both depending on its thermal characteristics [6, 7]. Including in the type of gel are N-isopropyl acrylamide (NIPA) gel and Poly (N-isopropyl acrylamide) gel which are also responsive to thermal changes. The gels can swell in aqueous solutions and absorb particular amount of the solution at temperatures below LCST. Likewise, the gels shrink and discharge the imbibed solution at temperature above the LCST. Further, drastically changes in volume are existed due to small increment/decrement of temperatures near their LCST [8,9]. Thermosensitive gel or thermoresponsive gel discussed here is a part of smart materials or smart polymers or smart hydrogels considered as polymeric system which is capable of responding to slightly changes in external medium including temperature: there is a transition temperature at which specific volume of the polymer drastically changes. Then, the changes also can affect several of its other properties such as coefficient of thermal expansion, heat conductivity, specific heat, and permeation [10].

The polymer gels as smart materials have attracted many concerns by scientists today due to their wide area of engineering applications including: drug delivery [11,12], enzyme or protein modification [13,14], biomedical applications: tissue barrier and tissue engineering. Besides, the smart gel also attracts many attention due to its wide range of potential applications as biomaterials for the care of wound pathologies [15], electro conductive natural polymer base hydrogels (ENPHs) for biosensors, artificial muscles, and wound healing [16-18], and some defense equipment: smart helmets, protective ballistic equipment [19], returnable water absorbing polymer [20], a smart sludge

dewatering system [21], sensors and transducers [22], actuators of microfluidic & small-size robotic devices [23,24], biomolecule-sensible [25], on-off switch of chemical reactions [26], etc. In conjunction with the polymer gels, polymeric aqueous solutions are also in high demands of research. Aqueous polymer solutions are considered as solutions which comprise particular amount of water and polymeric substances at particular concentrations which are diluted in it.

1.2 Objectives

The objectives of this work were to review factors affecting convective heat transfer inside a fluid-filled rectangular cavity, to study about fabrication technique of monodispersed spherical thermosensitive gels, specifically factors affecting diameter size of the resulted NIPA gels, to investigate swelling and shrinking phenomena of the NIPA gels at various diameters in a constant temperature fields and to clarify the dynamic behavior of the NIPA gels at various diameters inside an upper heating system of a rectangular cavity containing water and polymeric solution.

1.3 Structures of Dissertation

Structures of this dissertation can be described as follows: Chapter 1 is introduction part consisting of background, objectives, and structures of dissertation. Chapter 2 consists of review article and general theory and works from the previous researchers regarding convective heat transfer inside a fluid-filled rectangular cavity. Chapter 3 contains a research about generation of monodispersed thermo-sensitive gels and their swelling and shrinking behaviors inside water and polymeric aqueous solution. Chapter 4 represents general conclusions of this dissertation and recommendations for future works.

References:

1. T. Masuda, A.M. Akimoto, R. Yoshida, Self-Oscillating Polymer Materials, in M. Ebara (Ed), Biomaterials Nanoarchitectonics, Science Direct, 2016, 219-236.
2. Y. Bar-Cohen, Electroactive polymers as actuators, in K. Uchimo (Ed), Advance Piezoelectric Materials Science and Technology, Woodhead Publishing Limited, 2010, 287-317.
3. S-K. Ahn, R.M. Kasi, S-C. Kim, N. Sharma, Y. Zhou, Stimuli-responsive polymer gels, in Soft Matter, Royal Society of Chemistry, 2008, 4, 1151-1157.
4. M. Sobiech, P. Lulinski, Imprinted Polymeric Gels for Pharmaceutical and Biomedical Purposes, in V.K. Thakur, S.I. Voicu, M.K. Thakur (Eds), Polymer Gels: Perspective and Applications, Springer, 2018, pp.153-180.
5. D. Kumarasamy, M.K. Ghosh, T.K. Giri, Polymer-Based Responsive Hydrogel for Drug Delivery, in V.K. Thakur, S.I. Voicu, M.K. Thakur (Eds), Polymer Gels: Perspective and Applications, Springer, 2018, pp.1-152.
6. E.A. Clark, J.E.G. Lipson, LCST and UCST behavior in polymer solutions and blends, Polymer, 53, 2012, 536-545.
7. C. Wohlfarth, CRC Handbook of Liquid-Liquid Equilibrium Data of Polymer Solutions, 2008, CRC Press Taylor & Francis Group.
8. N. Zhang, S. Zheng, Z. Pan, Z. Liu, Phase Transition Effects on Mechanical Properties of NIPA Hydrogel, polymers, 10, 2018, 1-11.
9. H. Tokuyama, Y. Kato, Preparation of poly(N-isopropylacrymamide) emulsion gels and their drug release behavior, Colloids and Surfaces B: Biointerfaces, 67, 2008, 92-98.
10. M. Kutz, Mechanical Engineer's Handbook, 3rd Ed, 2006, John Wiley and Sons, Inc., Canada.

11. Y. Wei, K. Chen, L. Wu, In situ synthesis of high swell ratio polyacrylic acid/ silver nanocomposite hydrogels and their antimicrobial properties, Journal of Inorganic Biochemistry, 164, 2016, 17-25.
12. H.P James, R. John, A. Alex, K.R. Anoop, Smart polymers for the controlled delivery of drugs – a concise overview, Acta Pharmaceutica Sinica B, 4 (2), 2014, 120-127.
13. H. Murata, S. Carmali, S.L. Baker, K. Matyjaszewski, A.J. Russel, Solid-phase synthesis of protein-polymers on reversible immobilization support, nature communications, 2018, 9:845.
14. Y. Gong, J. Leroux, M.A. Gauthier, Releasable Conjugation of Polymers to Proteins, Bioconjugate Chemistry, American Chemical Society, 2015, 26, 1172-1181.
15. David C. Yeo, Polymeric Biomaterials for Management of Pathological Scarring, Applied Polymer Materials, 2019, 1, 612-624.
16. Z. Shi, X. Gao, M.W. Ullah, S. Li, Q. Wang, G. Yang, Electroconductive natural polymer-based hydrogels, Biomaterials, 2016, 111, 40-54.
17. J. Hur, K. Im, S.W. Kim, J. Kim, D. Chung, T. Kim, K.H. Jo, J.H. Hanh, Z. Bao, S. Whang, N. Park, Polypyrrole/ Agarose-Based Electronically Conductive and Reversible Restorable Hydrogel, ACS Nano, 8 (10), 2014, 10066-10076.
18. M. Talikowska, X. Fu, G. Lizak, Application of conducting polymers to wound care and skin tissue engineering: A review, Biosensors and Bioelectronics 135, (2019), 50-63.
19. J.G. Garrillo, R.A. Gamboa, E.A Flores-Johnson, P.I. Gonzalez-Chi, Ballistic performance of thermoplastic composite laminates made from aramid woven fabric and polypropylene matrix, Polymer Testing, 31, (2012), 512-519.
20. R.F.S. Frettas, E.L. Cussler, Chemical Engineering Science, 1987, 42, 97

21. T. Gotoh, H. Okamoto, S. Sakohara, Characterization and Swelling Behavior of Thermosensitive Porous Gel, Journal of Chemical Engineering Japan 2004, 37, 347.
22. K. Deligkaris, T.S. Tadele, W. Olthius, A. van den Berg, Hydrogel-based devices for biomedical applications, Sensors and Actuators B 2010, 147, 765.
23. W. Hilber, Stimulus-active polymer actuators for next-generation microfluidic devices, Applied Physics A, 2016, 122, 751.
24. L. Hines, K. Petersen, G.Z. Lum, M. Sitti, Soft Actuators for Small-Scale Robotics, Advanced Materials 2017, 29, 1603483.
25. S-H. Lee, T.H. Kim, M.D. Lima, R.H. Baughman, S. Kim, Biothermal sensing of a torsional artificial muscle, Nanoscale 2016, 8, 3248.
26. X. He, M. Aizenberg, O. Kuksenok, L.D. Zaizar, A. Shashtri, A.C. Balazs, Aizenberg, Journal of Nature 2012, 487, 214.

Chapter 2

Convective Heat Transfer inside a Fluid-Filled Rectangular Cavity

This chapter comprises contain from the International Journal of Applied Engineering Research published for publication in February 2018 Volume 13, Number 3.

Abstract

Heat transfer is one of interesting fields of research investigated in many engineering applications. It relates to the amount of energy transferred due to temperature difference of two or more surfaces of materials at a particular mode of transfer in respect of time. Heat transfer has several modes of delivery including convection, conduction, and radiation. Heat can be transferred through a medium or a combination of mediums which can be forms of solid, liquid, and gas or a combination of those forms. A number of researches have been carried out related to heat transfer concepts in a number areas of applications including energy, industry, health, etc. This research is to review on convective heat transfer inside a fluid-filled rectangular cavity and address a number of conditions affecting convective heat transfer of the systems including: effect of partially active wall, effect of nanoparticle fluid, effect of magnetic field, and effect of thermo-sensitive gels & functional particles. The conclusions are also presented based on the explanation of the information and data collected.

Keywords: Heat transfer, natural convection, negative thermal expansion, rectangular cavity, polymer solution, thermo-sensitive gel

Nomenclature

AR	aspect ratio
Bn	Bingham number
θ	angle of the rectangular cavity measured from the horizontal axis (°)
h	coefficient of heat transfer (kJ/m^{2}K)
ΔT	temperature difference of two opposing wall (K)
Ha	Hartmann number
H/L	height-length ratio (non-dimensional)
N	buoyancy ratio
Pr	Prandtl number
Ra	Rayleigh number
Nu	Nusselt number
θm	magnetic angle direction (°)

LCTS	Lower Critical Temperature Solution
NIPA	*N*-isopropylacrylamide
NTE	Negative Thermal Expansion
PAA	Polyacylamide Acid
PCM	Phase Change Material
SMA	Shape Memory Alloy

2.1 Introduction

Heat transfer is considered as one of interesting fields of research and its applications recently can be found in many engineering and commercial products including an electric blanket to maintain comfortable body temperature for post-surgery patients, environmentally friendly insulation materials for buildings and clothes in extreme weather conditions, hot furnaces for pig iron purification in steel industries, nuclear reactors, etc.

In general, heat can be transferred through several modes of delivery including convection, conduction, radiation, and variations of the modes through a medium or a combination of mediums which can be in forms of solid, liquid, and gas [1-3]. A number of research has been done so far by many scientists that investigate about natural convective heat transfer within particular fluids as a research interest including to observe the effect of active wall's position (heat source) and geometrical size of the cavity containing the fluids on some parameters of heat transfer such as temperature profiles, Nusselt number, and thermal conductivity. Convective heat transfer can be understood as heat transfer inside a medium having temperature difference due to the movement of the fluid which can be in forms of liquid or gas triggered by gravity and its density difference (natural convection) or the heat transfer is triggered by fluid motion having difference temperatures which can be generated by one or more external sources such as fan, compressor, and other devices (forced convection). Especially for natural convection, movement of the fluid is due to the interaction of gravity and density difference within the fluid affected by temperature differences, concentration, or composition [2].

Including natural convection within rectangular cavity is heat transfer between various surfaces of a rectangular parallelepiped cavity without interior solids defined by an angle term of θ measured from the horizontal. For this condition, fluid inside the cavity is

surrounded by two different parallel isothermal walls (upper and lower plates) that incline at the angle of θ from the horizontal and are separated at a particular distance (L). By terminology, term of $\theta = 0°$ is associated to horizontal plates heating from the below and term of $\theta = 90°$ is referring to vertical plates heating from the sides. For a particular condition, temperature of the upper plate can be higher than that of at the lower plate and for this condition, θ will equal to 180° that correlates to the horizontal wall heated from the above [2]. According to Bergman et al. [1], heat flux transversely through the fluid-filled cavity depends on convection heat transfer coefficient of the fluid (h) and difference temperatures of the two opposing walls (ΔT). In addition, an aspect ratio (H/L) and the value of θ described above also strongly affect heat flux of the cavity.

2.2 Effect of Partially Active Wall

Partially active wall refers to a condition where a heat source is located on one particular wall of the rectangular cavity. In fact, the rectangular cavity can have more than one heat sources mounted on its different wall. Some applications of the system can be found in heating and cooling of buildings, and cooling system of electronic heaters [4].

A number of research have been done especially based on this matter. Yigit et al. [5] investigated aspect ratios of the sample fluid which followed the model of Bingham fluid and studied about the influence of aspect ratio's parameters on natural convection inside rectangular enclosures heated from the below. In the research, aspect ratio of enclosure height (0.25 to 4) and nominal Rayleigh number (Ra = 103 to 105) for a single value of Prandtl number (Pr = 500) were set for the experiment. By comparing the Newtonian and Bingham fluids, it revealed that convective heat transfer was increasing with the increase of nominal Rayleigh number for the both fluids. In fact, the value of mean Nusselt number

of the fluids following the Bingham model remained smaller than that of the Newtonian fluids for the set values of *Ra* and *Pr*.

According to the research, it was due to increasing viscous resistance that occurred from yield stress in the Bingham fluids. Apparently, the mean Nusselt number decreased with the elevation of Bingham number (*Bn*) until thermal transfer was driven by conduction for larger values of *Bn*. In addition, effect of convection was weakening with the increasing of *AR* at a given value of *Ra* and *Pr* for both Bingham and Newtonian fluids. For *AR* above the values (i.e. for tall enclosures), the heat was mainly transferred by conductive mode of delivery.

A study about natural convection in rectangular cavities heated on one vertical wall where other five surfaces were considered adiabatic had been performed by Karatas & Derbentli [6]. In the research, aspect ratio (*A*) of each rectangular cavity was set to 1, 2.09, 3, 4, 5, and 6 respectively with a constant height of 340 mm and a depth of 210 mm. To obtain specific shape, length of cavity was varied according to a particular aspect ratio which referred to a height-length ratio (*H/L*). Thirty five positions of temperature distribution were set on the length direction and were vertically distributed in 3 positions: bottom, middle, and top. Only one line of temperature distribution was applied in respect to the depth of the cavity. The research revealed that slightly temperature changes near the central region and concentration of isotherms were formed near the active wall. In fact, local Nusselt number varied along the height of cavity for Rayleigh number ranging from 2.6 x 105 to 5.06 x 107. There were increasing temperatures from the left to the right wall and the temperature gradient at the left wall was higher than that of the right wall due to a local heat sink on the left wall. At the central area of the cavity, temperature profile showed a linear variation with lower temperature gradient compared to that of at the near wall region where the heat was transferred by a conductive mode of delivery.

Moreover, near the central area of the cavity, the temperature profile was almost flat for A=1 and A=2.09 but the gradient of temperature profile slightly increased with the increasing of aspect ratios (A) from 3 to 6. In case of the left wall for Y=0.125 (bottom line), temperature gradient was almost horizontal for all aspect ratios and it decreased when the aspect ratio was increased.

A numerical study of double-diffusive natural convection was investigated by Corcione et al. [7]. The research set vertical square enclosures having two opposite horizontal temperature and concentration gradient. The author solved conservation equations of energy, mass, momentum, and species by using computational codes based on SIMPLE-C algorithm for the combining pressure-velocity. In simulation of the experiment, some of independent variables were applied including buoyancy ratio, Lewis number, the Rayleigh number, and Prandtl number. The research revealed that mass and heat transfer were increasing if the Prandtl number and thermal Rayleigh number were expanded. Unlike the rate of mass transfer which was elevated with the augmented of Lewis number, heat transfer rate was fairly uncorrelated with the Lewis number provided that the buoyancy ratio was lower than the number at which the littlest heat transfer existed. Settings parameters of the experiment were performed for buoyancy ratio (N) ranging from 0.1 to 100, thermal Rayleigh number (RaT) ranging from 103 to 106, Prandtl (Pr) number ranging from 1 to 10, and Lewis number (Le) ranging from 1 to 1000.

The research showed that rate of heat transfer increased when RaT and Pr were augmented and effect of Pr number on heat transfer was less than that of RaT at higher number of buoyancy ratio (N). Other characteristics which worth to be addressed by the research was that the distribution of Nu Vs N, showed a minimum graph at Nusselt number equal to 1. Apparently, for Le = 1, the Nusselt number (Nu) exactly equal to unity and for Le > 1, Nu was only slightly higher than unity. At the value of N which was a

minimum, denoted by *NT-min*, there was a clockwise flow generated by the temperature gradient and the flow was then balanced by anti-clockwise fluid motion generated by opposed solutal gradient. As a result, motionless fluid was formed through which mass and heat was principally base on pure conduction. It also revealed that *NT-min* was increasing if both *RaT* and *Le* were increased. By this condition, the thickness of concentration boundary layer became thinner as the Lewis number elevated. Consequently, when solutal driving force expanded to develop thinner area of velocity boundary layer near to the cavity wall, the intensity of the solutal flow was decreasing and implied that higher buoyancy ratio was demanded to counteract the thermally-driven flow. What is more, flow generated by the temperature gradient remained more intense when the thermal Rayleigh number increased, and again, a higher buoyancy ratio was required to counteract it and the rate of heat transfer slightly depended on Lewis number for the buoyancy ratio lower than *NT-min*.

By considering aspect ratio (*AR*) of the enclosures, Nithyadevi et al. [8] performed a numerical study related to effect of the ratios on natural convection of a water-filled rectangular cavity. Active walls were on both vertical walls (temperature of the left wall was higher than that of the right wall) on which 9 non-identical positions were installed as a combination of heating and cooling pairs. The research revealed that if hot source was placed at the top side of the left wall and cold source was mounted on bottom of the right walls, there was no significant heat transfer occurred. Around the center of the cavity, heat transfer was dominated by conduction mode of delivery and convective heat transfer existed nearby the active walls. In fact, when hotter source was put on the bottom side of the vertical wall and colder source were mounted on the top side of another opposed vertical wall, then heat transfer rate was augmenting significantly as seen on Figure 1.

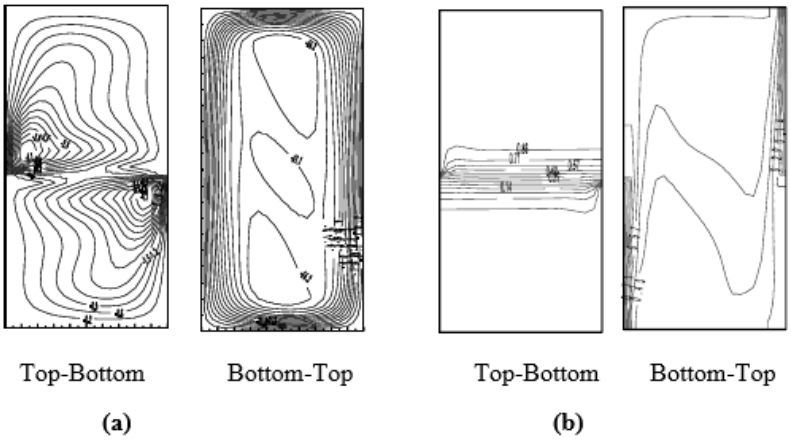

Figure 1. Stream Lines for AR = 2, Gr = 105 (a), and Isotherms Lines for AR = 2, Gr = 105 (b)

(Reprint from International Journal of Heat and Mass Transfer, with permission from Elsevier)

According to Kandaswamy et al. [9], natural convection occurred in a fluid-filled enclosure was due to the different density of the fluid triggered by dissimilar distribution temperatures of the fluid. Actually, most of assumptions used to describe temperature profile inside the cavity were based on a linear temperature-density relation. However, it was proved by the research that it was not exist in a real situation. Indeed, temperature-density's trend in practice was a non-linear pattern. In addition, position of heat source on the vertical wall also affected heat transfer rate inside the cavity.

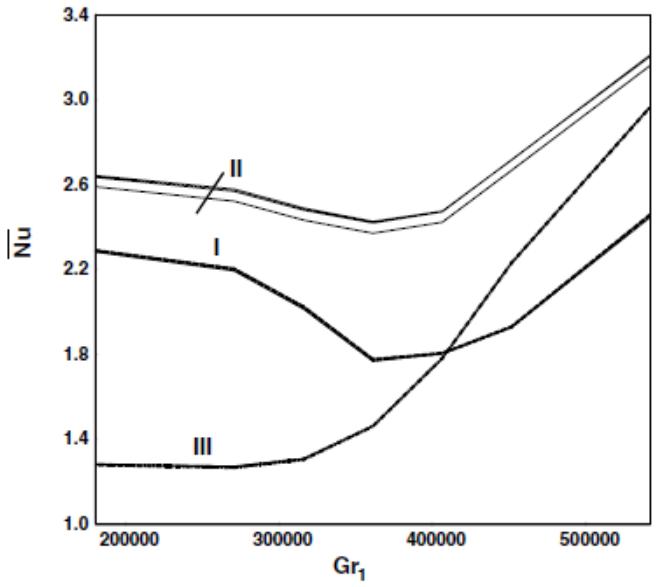

Figure 2. Relation of Grashorf Number and Average Nusselt Number

(Reprint from International Journal of Heat and Mass Transfer, with permission from Elsevier)

In case the hot source was mounted on left side of the cavity and the cold source was put on right side of the cavity, the important results of this research was that the heat transfer rate increased if heating source was placed at the middle of the hot wall and when the heat source was placed on the upper and the bottom area of the vertical cavity, heat transfer rate was less than that of at the middle of active wall.

The rate of heat transfer was decreasing up to the density maximum (at the lowest value of the average Nusselt number), and then heat transfer was increasing significantly with the increasing of the Grashof number for every position of the heat source (I, II, and III) as seen on Figure 2.

The rate of heat transfer was decreasing up to the density maximum (at the lowest value of the average Nusselt number) and then heat transfer was increasing significantly with the increasing of the Grashof number for every position of the heat source (I, II, and III) as seen on Figure 2. Sign I, II, and III represented positions of heat source on top, middle, and bottom of the active vertical wall respectively.

2.3 Effect of nanoparticle Fluid

The term of nanoparticle fluid or nano-fluid refers to the base fluid that has suspended nano-scale solid particles inside it without causing formation of sedimentation and has zero increase in pressure drop during the fluid flow [10-11].

Nano particle fluid or nanofluid has been investigated widely in laboratory and industrial scale as an alternative way to enhance convective heat transfer of any particular systems [12-15]. Hence, its application can be found mainly in heat exchangers, buildings heating, phase change materials, automotive cooling systems, and also in plants applications such as solar cells, solar collectors, nuclear reactor, micro-channels [15-16], etc.

The significance of this type of fluid being used as heat transfer agent has been studied by a number of researchers especially in convective heat transfer field of interest and has been investigated based on various interesting topics including: effect of inclined nanoparticle-filled enclosure [17-18], effect of volume fraction quantity of nanoparticle on temperature gradient, streamlines, and isotherm of the fluid [19], etc.

Heat transfer and flow of Al_2O_3-water nanofluid inside a square enclosure were investigated numerically and experimentally by Hu et al. [20]. The research revealed that heat transfer enhancement was only effective at the lower mass fraction of nanoparticles (1wt %) compared to the pure water and was almost constant at 2wt %. Additional nanoparticle mass fraction i.e. at 3wt %, led to reduction of heat transfer and these facts also concluded that for nanoparticle fluid, thermal conductivity was more dominant than viscosity in affecting heat transfer at low nanoparticle mass fraction. In fact, heat transfer was more influenced by viscosity than thermal conductivity at higher fraction of nanoparticle fluid.

Contrast to the above results, similar nanoparticle fluid (alumina-water) was also investigated by Ho et al. [21] by considering thermal conductivity and unpredictability in effective dynamics viscosity of nanofluid in respect to natural convective heat transfer inside a square cavity. This research revealed that additional nanofluid inside the base fluid did not always increase heat transfer performance as it depended basically on the formula used in determining the effective dynamic viscosity and the Rayleigh number. Conductive heat transfer dominated through the alumina-water filled rectangular cavity at *Ra* equal to 1000, this condition led to the fact that increasing the amount of alumina volume fractions could increase the average Nusselt number reflecting an enhancement of thermal conductivity of the nanofluid. In fact, for higher value of Rayleigh number ($Ra \geq 104$), heat transfer across the cavity was dominated by convection mode and average

Nusselt number showed increasing and decreasing patterns with the particle volume fractions for model I-III and model II-IV respectively. The difference between these two models curves was due to the difference of effective dynamic viscosity enhancement of the fluid extracted from two adopted formulas used to determine Nusselt number.

In respect to the dispersion of nanoparticles inside the fluid-filled cavity, Celli [22] proposed the possibility of a non-homogenous model to study spatial distribution of the nanoparticles inside the cavity and to investigate heat transfer performance of the fluid in respect to a natural convection phenomenon. Based on this research, non-homogenous distribution of nanoparticle occurred at lower values of Rayleigh number. In fact, fairly homogenous distribution was established in the core of the cavity at the Rayleigh number higher than 100. Similar to other research, the increasing of volume fraction of nanoparticle led to the decreasing of heat transfer at the vertical boundary.

Regarding the position of the enclosure, a research on an incline rectangular cavity was investigated by Bouhalleb et al. [23] that investigated about the correlation between Rayleigh number (*Ra*) and nanofluid flow pattern by applying various low aspect ratios (AR = 0.5, 0.25, 0.125, 0.1, 0.08) on the CuO-water nanofluid filled cavity cooled from the above and heated from one side of another wall. Aspect ratio of this case referred to a ratio of cold wall and hot wall surface. Based on the research, effect of Ra number was less significant to heat transfer for lower value of the aspect ratios. In fact, significant effect of heat transfer was clearly seen for higher aspect ratio and higher number of *Ra*. In addition, increasing of nanoparticle volume fractions led to increasing heat transfer performance significantly. If the dilute nanofluid concentration was set at 4% and at a value slightly greater than 2.5%, coefficient of heat transfer was increasing by 5% and 25 % respectively comparable with the pure water.

Inclination of the cavity also provided trends to heat transfer's coefficient in respect to volume fraction of nanofluid particles as seen on Figure 3. It described that heat transfer was gradually increasing until reaching a maximum point at a correlated inclination angle and then decreased moderately with the increasing of inclination angles.

This effect had the highest value of Nusselt number (*Nu*) at 2% of nanofluid concentration with an inclination angle of 30° and then lower values were represented by concentration of 4% and 0% (pure water) respectively. In addition, effect of aspect ratio was in great difference between the tall and the shallow cavity. Observation of 2% nanofluid concentration without applying inclination angle showed that, for lower *AR* (tall cavity), great slopes of *Nu*-*AR* curves were obtained for every particular of observed Rayleigh numbers. Contrarily, slopes of the curves were decreasing as the *AR* numbers were augmented. This fact showed that effect of convective heat transfer in the tall cavity was greater than that of in the shallow cavity.

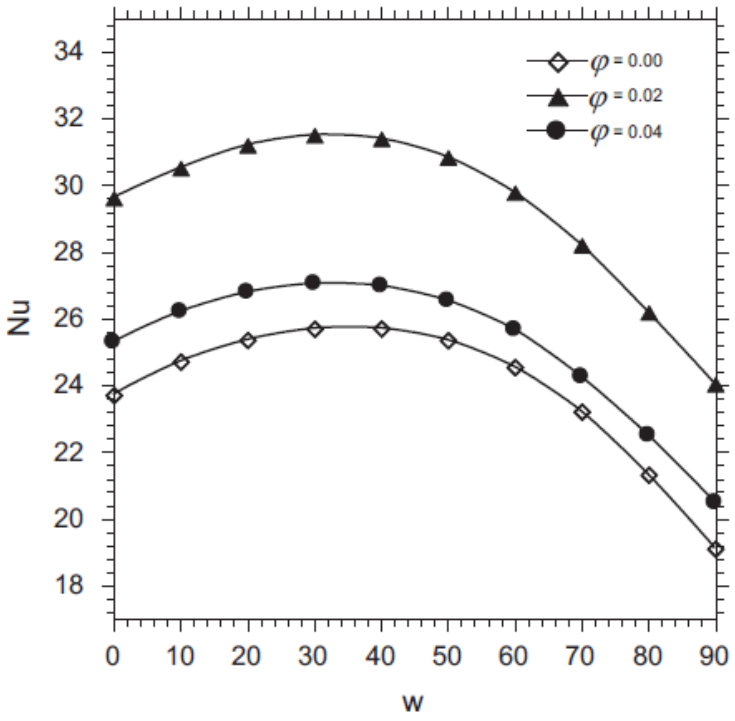

Figure 3. Nusselt Number and Inclination Angle for Various Volume Fractions at Ra = 107 and AR = 0.1
(Reprint from International Journal of Hydrogen Energy, with permission from Elsevier)

2.4 Effect of Magnetic Field

Effect of magnetic field has been considered as a significant factor affecting the rate of heat transfer inside the cavity and this fact has led to a complementation of magnetic field to fluid-filled systems as it could be found in engineering applications such as cooling mechanism of electronic components, combustion modelling, fire engineering, heat exchanger, and nuclear reactor [24]. Related studies have been done that used magnetic fields as a means of controlling crystal growth and structure development in the crystallization of alloys affected by convective heat transfer of the melting alloys [25]. In addition, a number of research also have been done regarding effects of magnetic field on heat transfer performance of a fluid-filled system including: effect of using magnetic-sensitive nanofluid and rotating magnetic field [26], implementation of Fe_3O_4 ferro-fluids interfered with single or double sources of magnetic field [27], magnetic nanofluid flowing inside circular pipe heated with a uniform magnetic field [28], interferences of constant and alternating magnetic field having two different intensities on convective performance of Fe3O4-water fluid inside a heated tube [29], etc.

Shaikholeslami et al. [30] investigated behavior of Fe_3O_4-water nanofluid in a cavity provided with a sinusoidal cold-wall under the influence of external magnetic field by considering effect of the ferro-fluid's volume fraction, Hartmann number (*Ha*) and Rayleigh number (*Ra*). The research revealed that, if the distance of hot and cold wall was shortened (i.e. higher value of cold wall's amplitude), temperature gradient of the fluid increased significantly under low effect of buoyancy force. In addition, by increasing Lorentz forces, which was related to higher number of *Ha* due to the increasing of magnetic field, average Nusselt numbers (Nu_{ave}) tended to decrease because the fluid velocity became retarded and conduction mode of delivery dominated the heat transfer.

In fact, as the buoyancy forces and Rayleigh number increased, average Nusselt number was raising and the temperature gradient closed to the right wall was augmented.

Effect of a uniform magnetic field to buoyancy driven convective heat transfer inside a rectangular enclosure was investigated by Wang et al. [31]. The research showed that at the beginning, Nusselt number was increasing for the lowest value of Hartmann number (*Ha*) until it reached the peak before decreasing again with the increasing of Hartmann number. This behavior was applied to all the three Grashof number selected in the experiment: the lowest Grashof number represented the lowest Nusselt number for all range of Hartmann numbers. A correlation between vertical velocity of the fluid (*v*) and magnetic field intensity (*Ha*) was also identical to that of *Nu* and *Ha* number. Similar to the previous study by [29], Lorentz forces due to the induced current could cause deceleration of liquid metal flow inside the cavity. Effective heat transfer was only obtained from moderate Hartmann number (*Ha* = 211.91) where energy transport process was more effective. For further increasing of Hartmann number, the fluid velocity became more stagnant and pure conduction of heat transfer then existed. In addition, externally imposed magnetic field was investigated by Oreper and Szekely [32]. The research revealed that natural convection could be restrained by magnetic fields depending on the intensity of magnetic field, geometry and size of the system. The presence of external magnetic field could change temperature and velocity fields with the provision of large magnetic fields. If the magnetic fields were set transversal to the gravitational force, the induction slightly greater than hundreds Gauss would cause apparent effects on the patterns of temperature and velocity of the observed system.

Complement to the above results, Gangawane [33] investigated effect of magnetic field's angle and heater size on free convection inside an open ended enclosure having one vertically left active wall. The research revealed that magnetic field applied at 45° of

the normal provided the highest constraint effect on convective heat transfer comparable to that of 0° and 90°. In more specific, heater size (*LH*), Hartmann number and Rayleigh number were set equal to 0.25, 50 and 103 respectively. For this condition, buoyancy force was obviously small and conductive mode of delivery dominated convection of heat transfer. The flow structures separated into two areas: one main region circulated near heated wall and the other minor region flowed near the open end of the enclosure. Obviously, when *Ra* number was raised up to 1000, by setting a higher power of the heat source, circulation flow of the fluid moving in from the open end existed. The flow then reached the hot wall before flowing out again to the open end surface. In fact, this circulation was limited toward walls' surfaces and caused a vortex in the middle of enclosure. In addition, by increasing the heater size to $LH = 0.5$ and $LH = 0.75$, buoyancy force became strong supporting the fluid to circulate throughout the enclosure. Significant changes existed for magnetic angle direction (θm) of 45° as circulating flow patterns were more skewed to the heated wall and secondary vortex existed near the open end. As a result, split fluid zones formed in the between and caused stagnant motion of fluid in the middle of cavity. This fact indicated that effect of Lorentz forces due to magnetic fields were maximum for this angle and provided the highest restriction to convective heat transfer.

2.5 Effect of Thermo-sensitive Gel and Functional Particle

Thermo-sensitive gel can be used as a heat transfer agent due to its sensitivity to the very low environment temperature changes. The gel can be utilized to several applications including drugs delivery system in the human body as the material can be transformed from liquid to gel at the near human body temperature [34], artificial scaffold inside human's tissues to trigger growth of the new bone [35-37], smart material for flow control

and mechanical micro-valve [38-39]. Terminology of 'gel' refers to a soft-solid-like material which consists of a number of components including polymeric materials and aqueous fluid presented in a substantial amount of quantity [40]. One type of thermo-sensitive gel, Poly (*N*-isopropylacrylamide), has LCTS at around 32°C that could be determined by the temperature where a dramatic volume change begins to occur [41].

The role of thermo-sensitive gel as a heat transfer agent is supported by its swelling-shrinking characteristic (i.e. swelling ratio) affected by internal properties and external stimuli such as crosslinking density [42], pores size [43], temperature changes of its surroundings fluid, salt concentration [44], UV radiation, and alkalinity (*pH*) of solutions [45].

Behavior of thermo-sensitive gel has been investigated by Hasegawa et al. [46] at Kanazawa University and some of related results could be depicted from Figure 4 that showed the appearance of NIPA gels inside the cavity within the interval of 1 minute and represented the condition of 145 minutes after the commencement of the recorded data. Thermocouple was mounted at the left side of the wall inside the cavity to measure the middle point temperature which was observed stable at 25°C.

Location of the four particles observed i.e. A, B, C, and D can be clearly seen corresponding to red, yellow, blue, and green circle respectively. Observation of the gels showed that the gels maintained repetitive movements in up and down direction in the certain period of time inside the rectangular cavity heated from the above and cooled from the below as shown on Figure 4. When the gels swelled at near the hot top surface of the cavity, the gels absorbed the heat and caused the diameter of the gels became larger because particular amount of solution was absorbed by the NIPA gels.

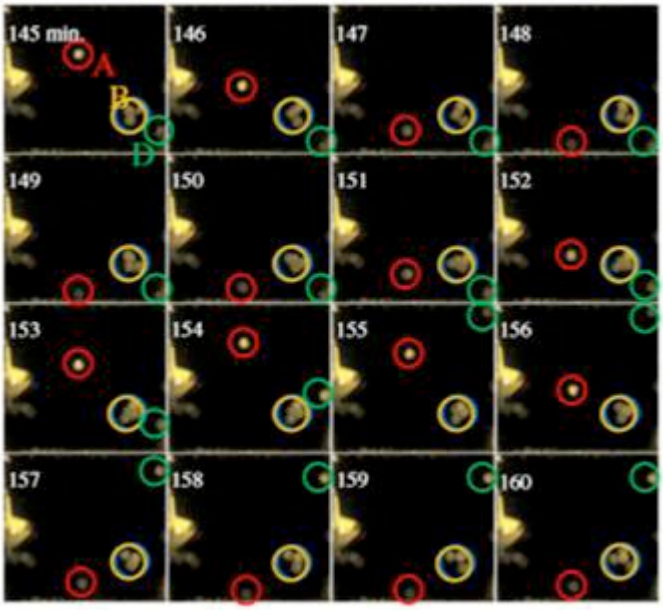

Figure 4. Gels Particles Movement inside the Rectangular Cavity

(Reprint from International Communications in Heat and Mass Transfer, with permission from Elsevier)

As a result, density of the gels became larger than that of surrounding PAA solution and immediately caused the gels to be shrinking and dropped to the bottom area i.e. cold area of the cavity. During the shrinking process until the gels were reaching at the bottom cold surface of the cavity, NIPA networks blocked the PAA polymer solution preventing it to penetrate the NIPA network. As a consequence, density of the gels became smaller than that of surrounding solution and this phenomenon created a buoyancy force on the surface of the gels and pushed the gels to move upward. The up and down movements would still continue provided the density differences existed between the gels and the polymer solution.

In case of a fluid-filled cavity where the hot wall was on the upper side and the cold wall was on the below, application of such thermo-sensitive gels could boost the intermixture of hot and cold fluid region. As a consequence, it could support convective heat transfer inside such a condition. The size of the gels being used also could affect

dynamics of gels inside the cavity and according to Tanaka et al. [47], the rate of response was actually inversely correlated with the square size of the gels.

Functional particles also could be applied as a heat transfer agent and could increase convective heat transfer rate [48]. The functional particles behaved contrary to the common materials when heated and exhibited inversely thermal expansion behavior as the material contracted and shrank its volume when heated. Including in this type of functional particles are negative thermal expansion (NTE) capsule applying phase change material (PCM) and shape memory alloy (SMA) particles.

Regarding the shape memory alloy particles, Kataoka & Yoshida [49] proposed particle implementing SMA spring inside the particle to promote natural convection within the thermally stratified fluid region of the rectangular cavity. By using the particles, natural convection existed in the inverse direction i.e. the hot fluid moved down and the cold fluid went up due to the back and forth movements of the functional particle. The experiment showed significant difference of temperature profile along the vertical height of the cavity when comparing case 1 (without functional particle) with case 2 (with functional particle). The slope of temperatures in the case 2 was greater than that of in the case1 and the stratified fluid region diminished gradually.

In addition to the above results, Yamaguchi and Takanashi [50] promoted NTE capsule supported with PCM (L-Type and S-Type). The research revealed that the movements of NTE Capsule inside the one-meter-depth of water tank were influenced by temperature contour of the ambient water by which could affect density of water and buoyancy force acting on the NTE Capsule. In principal, when the particle was in the hot fluid region, steam pressure of PCM (using RC318) inside the smaller cylindrical vessel elevated significantly and pressed the larger cylindrical vessel filled with pressurized air. Thus, the larger cylindrical vessel became shorten but the cumulative length of the both

vessels was kept on the constant automatically. As an effect, volume of the larger vessel decreased significantly when the temperature raised and decreasing its buoyancy force acting on the vessel. This fact triggered the NTE Capsule to move down and exhibited a negative thermal expansion.

2.6 Conclusions

A number of research have been reviewed in respect to convective heat transfer phenomena inside a fluid-filled rectangular cavity and have contributed to some significant factors affecting the heat transfer performance. Effect of partially active wall, effect of magnetic fields, and effect of applied thermo-sensitive gels and functional particles were investigated for this purpose. It was obvious that position of heat source along the vertical wall and the heat source facing direction on the horizontal axis as well as its intensity could affect performance of convective heat transfer inside the cavity. Direction, continuity, and intensity of applied magnetic field also had apparent effects on the convective heat transfer performance. The applied of thermo-sensitive gels and functional particles obviously could support natural convection of heat transfer inside thermally-stratified fluid region of the rectangular cavity.

Acknowledgement

The authors thank to Kanazawa University (KU), Japan and Ministry of Research, Technology and Higher education (KEMRISTEKDIKTI) of Indonesian Government for the existing bilateral academic-cooperation. An appreciation is also granted to Indonesia Endowment Fund for Education (LPDP) that provides fund through a BUDI-LN Scholarship Scheme.

References

[1] Bergman, L.T., Lavine, S.A., Incopera, P.F., and Dewitt P.D., 2009, "Heat and Mass Transfer", 7th Edition, John Willey & Sons Publisher, USA.

[2] Rohsenow, W.M., Hartnett, J.P., and Cho, Y.I., 1998, "Handbook of Heat Transfer", 3th Edition, McGraw-Hill, New York.

[3] Holman, J.P., 2010, "Heat Transfer", Tenth Edition, McGraw-Hill, New York.

[4] Oztop, H.F., and Abu-Nada, E., 2008, "Numerical Study of Natural Convection in Partially Heated Rectangular Enclosures Filled with Nanofluids", International Journal of Heat and Fluid Flow, 29, pp. 1326–1336.

[5] Yigit, S, Poole, R.J., and Chakraborty, N., 2015, "Effect of Aspect Ratio on Natural Convection of Bingham Fluids in Rectangular Enclosure with Differentially Heated Horizontal Walls Heated from Below", International Journal of Heat and Mass Transfer, Vol. 80, pp 727-736.

[6] Karatas, H., and Derbentli, T., 2017, "Natural Convection in Rectangular Cavities with One Active Vertical Wall", International Journal of Heat and Mass Transfer, Vol.105, pp. 305-315.

[7] Corcione, M., Grignaffini, S., and Quintino, A., 2015, "Correlation for the Double-diffusive Natural Convection in Square Enclosures Induced by Opposite Temperature and Concentration Gradient", International Journal of Heat and Mass Transfer, Vol. 81, pp. 811-819.

[8] Nithyadevi, N., Kandaswamy, P., and Lee, J., 2007, "Natural Convection in a Rectangular Cavity with Partially Active Side Walls, International Journal of Heat and Mass Transfer, Vol. 50, pp.4688-4697.

[9] Kandaswamy, P., Sivasankaran, S., and Nithyadevi, N., 2007, "Buoyancy-driven Convection of Water Near Its Density Maximum with Partially Active Vertical Walls, International Journal of Heat and Mass Transfer, Vol. 50, pp. 942–948.

[10] Abu-Nada, E., 2008, "Application of Nanofluids for Heat Transfer Enhancement of Separated Flows Encountered in a Backward Facing Step", International Journal of Heat and Fluid Flow, Vol. 29, pp. 242–249.

[11] Daungthongsuk, W., and Wongwises, S., 2007, "A Critical Review of Convective Heat Transfer Nanofluids", Renewable and Sustainable Energy Reviews, Vol. 11, pp. 797–817.

[12] Yu, G., Gao, D., Chen, J., Dai, B., Liu, D., Song, Y., and Chen, X., 2016, "Experimental Research on Heat Transfer Characteristics of CuO Nanofluid in Adiabatic Condition," Journal of Nanomaterials, Vol. 2016, pp. 1-7.

[13] Kuznetsov, A.V., and Nield, D.A., 2010, "Natural Convective Boundary-layer Flow of a Nanofluid Past a Vertical Plate", International Journal of Thermal Sciences, Vol. 49, pp. 243–247.

[14] Coudhury, P., Garg, P., and Jha, S., 2014, "Study of Nano Particles for Enhanced Heat Transfer Characteristics of Base Fluids for Cool Thermal Energy System", International Journal of Engineering Research and Applications, Vol. 4 (4), pp. 97-101.

[15] Das, S.K., Choi, S.U.S., and Patel, H.E., 2006, "Heat Transfer in Nanofluids-A Review", Heat Transfer Engineering, Vol. 27(10), pp. 3–19.

[16] Mansour, M.A., Mohamed, R.A., Abd-Elaziz, M.M., and Ahmed, S.E., 2010, "Numerical Simulation of Mixed Convection Flows in a Square Lid-driven Cavity Partially Heated from Below Using Nanofluid", International Communications in Heat and Mass Transfer, Vol. 37, pp. 1504–1512.

[17] Heris, S.Z., Pour, M.B., Mahian, O., and Wongwises, S., 2014, "A comparative Experimental Study on the Natural Convection Heat Transfer of Different Metal Oxide Nanopowders Suspended in Turbine Oil Inside an Inclined Cavity", International Journal of Heat and Mass Transfer, Vol. 73, pp. 231–238.

[18] Abu-Nada, E., and Oztop, H.F., 2009, "Effects of Inclination Angle on Natural Convection in Enclosures Filled with Cu–water Nanofluid", International Journal of Heat and Fluid Flow, Vol. 30, pp. 669–678.

[19] Khanafer, K., Vafai, K., and Lightstone, M., 2003, "Buoyancy-driven Heat Transfer Enhancement in a Two-dimensional Enclosure Utilizing Nanofluids", International Journal of Heat and Mass Transfer, Vol. 46, pp. 3639–3653.

[20] Hu, Y., He, Y., Qi, C., Jiang, B., and Schlaberg, H.I., 2014, "Experimental and Numerical Study of Natural Convection in a Square Enclosure Filled with Nanofluid", International Journal of Heat and Mass Transfer, Vol. 78, pp. 380–392.

[21] Ho, C.J., Chen, M.W., and Li, Z.W., 2008, "Numerical Simulation of Natural Convection of Nanofluid in a Square Enclosure: Effects Due to Uncertainties of Viscosity and Thermal Conductivity", International Journal of Heat and Mass Transfer, Vol. 51, pp. 4506–4516.

[22] Celli, M., 2013, "Non-homogeneous Model for a Side Heated Square Cavity Filled with a Nanofluid", International Journal of Heat and Fluid Flow, Vol. 44, pp. 327–335.

[23] Bouhalleb, M., and Abbassi, H., 2014, "Natural Convection of Nanofluids in Enclosures with Low Aspect Ratios", International Journal of Hydrogen Energy, Vol. 39(27), pp. 15275-15286.

[24] Hassan, A.R., and Maritz, R., 2016, “The Analysis of a Reactive Hydromagnetic Internal Heat Generating Poiseuille Fluid Flow through a Channel”, SpringerPlus, Vol. 5(1):1332.

[25] Mikelson, A.E., and Karlin, Y.K., 1981, “Control of Crystallization Processes by Means of Magnetic Fields”, Journal of Crystal Growth, Vol. 52, pp. 524-529.

[26] Fadaei, F., Dehkordi, A.M., Shahrokhi, M., and Abbasi Z., 2017, “Convective-heat Transfer of Magnetic-sensitive nanofluids in the Presence of Rotating Magnetic Field”, Applied Thermal Engineering, Vol. 116, pp. 329–343.

[27] Fadaei, F., Shahrokhi, M., Abbasi, Z., Dehkordi, A.M., and Abbasi, Z., 2017, “Heat Transfer Enhancement of Fe3O4 Ferrofluids in the Presence of Magnetic Field”, Journal of Magnetism and Magnetic Materials Vol. 429, pp. 314–323.

[28] Hatami, N., Banari, A.K., Malekzadeh, A., and Pouranfard, A.R., 2017, “The Effect of Magnetic Field on Nanofluids Heat Transfer Through a Uniformly Heated Horizontal Tube”, Physics Letters A, Vol. 381, pp. 510–515.

[29] Goharkhah, M., Salarian, A., Ashjaee, M., and Shahabadi M., 2015, “Convective Heat Transfer Characteristics of Magnetite Nanofluid under the Influence of Constant and Alternating Magnetic Field, Powder Technology Vol. 274, pp. 258–267.

[30] Sheikholeslami, M., and Ganji, D.D., 2016, “Ferrofluid Convective Heat Transfer under the Influence of External Magnetic Source”, Alexandria Engineering Journal.

[31] Wang, Z.H., Meng, X., and Ni, M.J., 2017, “Liquid Metal Buoyancy Driven Convection Heat Transfer in a Rectangular Enclosure in the Presence of a Transverse Magnetic Field”, International Journal of Heat and Mass Transfer, Vol. 113, pp. 514–523.

[32] Oreper, G.M., and Szekely, J., 1983, "The Effect of an Externally Imposed Magnetic Field on Buoyance Driven Flow in a Rectangular Cavity", Journal of Cristal Growth, Vol. 64, pp. 505-515.

[33] Gangawane, K.M., 2017, "Effect of Angle of Applied Magnetic Field on Natural Convection in an Open Ended Cavity with Partially Active Walls", Chemical Engineering Research and Design, Vol. 127, pp. 22–34.

[34] Hoare, R.T., and Kohane S.D., 2008, "Hydrogel in drug delivery: Progress and Challenges", Polymer, Vol. 49(8), pp. 1993-2007.

[35] El-Sherbiny, I.M., Yacoub, M.H., 2013, "Hydrogel Scaffolds for Tissue Engineering: Progress and Challenges", Global Cardiology Science and Practice, Vol. 38, pp. 316-342.

[36] Ziane, S., Schlaubitz, S., Miraux, S., Patwa, A., Lalande, C., Bilem, I., Lepreux, S., Rousseau, B., Meins, J.L., Latxague, L., Barthélémy, P., and Chassande, O., 2012, "A Thermosensitive Low Molecular Weight Hydrogel as Scaffold for Tissue Engineering", European Cells and Materials, Vol. 23, pp. 147-160.

[37] Tozzi, G., Mori, A.D., Oliveira, A., and Roldo, M., 2016, "Composite Hydrogels for Bone Regeneration", Materials, Vol. 9(4), 267; doi: 10.3390/ma9040267.

[38] Arndt, K., Kuckling, D., and Richter, A., 2000, "Application of Sensitive Hydrogels in Flow Control", Polymers for Advance Technologies, Vol. 11, pp. 496-505.

[39] Baldi, A., Gu, Y., Loftness, P.E., Siegel, R.A., and Ziaie, B., 2003, "A Hydrogel-actuated Environmentally Sensitive Microvalve for Active Flow Control", Journal of Microelectromechanical Systems, Vol. 12(5), pp. 613-621.

[40] Bromberg, L.E., and Ron, E.S., 1998, "Temperature-responsive Gels and Thermogelling Polymer Matrices for Protein and Peptide Delivery, Advance Drug Delivery reviews, Vol.31, pp. 197-221.

[41] Wang, H.D., Chu, L.Y., Yu, X.Q., Xie, R., Yang, M., Xu, D., Zhang, J., and Hu, L., 2007, Thermosensitive Affinity Behaviour of Poly(N-isopropylacrylamide) Hydrogel with *ß* Cyclodextrin Moieties, Ind. Eng. Chem. Res. Vol. 46, No.5.

[42] Oh, K.S., Oh, J.S., Choi, H.S., and Bae, Y.C., 1998, "Effect of Cross-Linking Density on Swelling Behavior of NIPA Gel Particles", Macromolecules, Vol. 31, pp. 7328-7335.

[43] Yacob, N., and Hashim, K., 2014, "Morphological Effect on Swelling Behavior of Hydrogel", AIP Conference Proceedings 1584, 153; 10.1063/1.4866123

[44] Mirdarikvande, S., Sadeghi, H., Godarzi, A., Alahyari, M., Shasavari, H., Khani, F., 2014, "Effect of pH, and Salinity onto Swelling Properties of Hydrogels Based on H-alginate-g-poly (AMPS)", Biosciences Biotechnology Research Asia, Vol. 11(1), pp. 205-209.

[45] De, S.K., Aluru, N.R., Johnson, B., Crone, W.C., Beebe, D.J., and Moore, J., 2002, "Equilibrium Swelling and Kinetics of pH-Responsive Hydrogels: Models, Experiments, and Simulations", Journal of Microelectromechanical Systems, Vol. 11, No.5.

[46] Hasegawa, M., Kamikido, T., Kawabata, N., 2016, "Behavior of Thermosensitive Gel in Polymer Solution", International Communications in Heat and Mass Transfer, Vol. 76, pp. 55-58.

[47] Tanaka, T., and Fillore, J., J. Chem. Phys. 1979, 70, 1214.

[48] Zhang, Y., Rao, Z., Wang, S., Zhang, Z., Li, X., 2012, "Experimental Evaluation on Natural Convection Heat Transfer of Microencapsulated Phase Change Materials Slurry in a Rectangular Heat Storage Tank", Energy Conversion and Management, Vo. 59, pp. 33-39.

[49] Kataoka, I., Yoshida, K., 2002, “Development of Inverse Natural Convective Fluid and Its Thermo-hydrodynamics Characteristic”, Experimental Thermal and Fluid Science, Vol. 26, pp. 345-353.

[50] Yamaguchi, Y., and Takanashi, K., 2004, “Estimation of Buoyancy Change of an NTE Capsule Using PCM”, Proceedings of ASME International Mechanical Engineering Congress and Exposition, Anaheim, California USA.

Chapter 3

Fabrication of Monodispersed Spherical Thermo sensitive Gels and Their Swelling and Shrinking Behaviors in Aqueous Polymeric Solution

This chapter contains a research article published in *Applied Sciences*, a Science Citation Indexed journal, published in Volume 10, Issue 6, 2020.

3.1 Introduction

Every material demonstrates a thermal response to temperature changes in its surroundings; therefore, a material's behavior could vary under different conditions. Most materials exhibit positive thermal expansion at high temperatures, although some materials may demonstrate negative thermal expansion. Thermosensitive gels are one such material; they shrink when submerged in high-temperature liquids such as aqueous polymeric solutions and then swell when submerged in cooler fluids. The thermosensitive gels used in this study were generated in a laboratory for application specifically in the upper heating system (or the lower cooling system) of a rectangular enclosure. Such systems have a disadvantageous property that limits heat transfer between two opposite horizontal walls; however, they offer an advantage: When thermosensitive gels and a polymeric solution fill the gap between the two opposite heat sources, the gels show distinctive mechanical behaviors of repetitive shrinking and swelling over a period of time. The system used in this study comprises N-isopropyl acrylamide (NIPA) gels and sodium polyacrylate (PAANa) solution in an integrated system; these materials form the focus of this study's observations. Theoretically, an aqueous polymeric solution is considered as an aqueous fluid comprising water and polymeric substances at a certain concentration. Polymeric solutions are important because of their application in multiple pharmaceutical and biomedical contexts [1] such as drug delivery [2] and enzyme or protein modifications [3,4].

Currently, thermosensitive gels have attracted considerable attention because they can be created using physical or chemical cross-linkers and form a unique class of polymeric materials that can retain quantities of water while maintaining their own structures [5]. Thermosensitive gels may be in either a sol or a gel phase depending on their temperature.

The sol phase is considered as a fluid state, whereas the gel phase is related to a rigid, non-fluid state in which the shape/physical structure is preserved. Typically, the sol–gel state can be achieved only via a thermal stimulus. For biomedical applications, the condition is suitable for in situ hydrogel formation at close to human-body temperature without requiring additional chemical initiators [6].

Theoretically, depending on its thermal characteristics, a thermosensitive gel may have either a lower critical solution temperature (LCST) or an upper critical solution temperature [7,8]. NIPA gel swells in aqueous solutions and absorbs a certain amount of the solution at temperatures below its LCST. At temperatures above its LCST, the gel shrinks and discharges the absorbed solution. Moreover, significant changes in volume occur because of small temperature changes close to the gel's LCST [9–11]. Exposing NIPA gel to a monotonic load above its LCST reveals a tougher mechanical behavior than is evident below its LCST in terms of nominal stress, stretch, and Young's modulus. This makes the gel suitable for health applications such as the regeneration of damaged tissues [12]. Furthermore, when NIPA gels are submerged in an aqueous polymer solution in a rectangular cavity, they exhibit repetitive vertical motions for a certain length of time [13]. Hasegawa et al. used a polymeric solution (polyacrylamide [PAA]) as a fluid for surrounding the gels because its density is between those of the gels in their swollen and shrunken states. When the gels were heated in the upper layer, they began to shrink, their volume decreased, and their density increased above that of the surrounding fluid. Consequently, the gels slowly moved toward the bottom of the cavity. Similarly, when the gels were cooled in the cavity's lower layer, the gels started to swell, their volume increased, and their density became lower than that of the surrounding fluid; hence, the gels moved upward. These conditions enabled the gels to vertically move in cyclical motions. They used cylindrical-shaped thermosensitive gels that were flat on both sides.

One of the gels showed a vertical motion frequency of one cycle per 10 min for a duration of 230 min within a PAA solution. Other gels became easily attached to each other; they frequently adhered to the walls of the rectangular cavity, which promptly stopped their vertical movements because of the large contact areas on their flat sides. However, observations of NIPA gel behavior within an upper heating rectangular cavity have not received considerable attention, and literature on this topic is quite limited. Oh et al. revealed that for NIPA gel particles that are smaller than 200 nm, as their cross-linking density decreases, the volume change of the NIPA particles becomes more discontinuous [14]. This result corresponds with that obtained by Tanaka and Li [15]. Furthermore, the behavior of the gels at lower temperatures of about 20 °C demonstrates that those gels with a lower cross-linking density tend to have higher swelling rates than those with higher cross-linking densities. In fact, the temperature at which the gels start to swell is higher for those gels with higher cross-linking densities [14]. Moreover, the swelling behavior of NIPA gels is enhanced by increasing the gels' porous structures [16–19]. The addition of an initiator, such as dodecyl dimethyl benzyl ammonium bromide (DDBAB) and ammonium persulfate (APS), produced a hydrophobic initiator, dodecyl dimethyl benzyl ammonium persulfate, which provides a heterogeneous initiation mechanism and triggers the development of macro-porous structures [18] and an increased temperature response in the gel, as reported by Zhao et al. [18,19].

Recently, NIPA gels of various shapes and sizes have been produced. To minimize size variations, monodispersed spherical-shaped gels are generally made in laboratory scales using microfluidic devices [20–25]. The droplet diameter is controlled by adjusting the droplet-breakup mechanism, which is affected by the capillary number of the continuous-phase flow [26–28]. Previously, studies have reported that increases in flow-rate ratios and capillary numbers correspond to a significant decrease in droplet diameter

[29,30]. The flow rate of the continuous phase plays a significant role in controlling droplet size. A reduced flow rate in the continuous phase affects the neck length, current contact angle, and mean drop-growth velocity, which in turn affects droplet formation [31]. Other studies highlight the significant effect of interfacial tension on droplet size [32,33]. Furthermore, density differences between the continuous-phase flow and the dispersed flow affect the formation of the droplet's diameter as has been explained by Scheele et al. [34]. Based on research by Leong et al., by implementing two different diameters of a capillary tube for a constant velocity of the dispersed-phase flow, the droplet-size formation in both tubes decreased as the continuous-phase flow velocity increased. In their study, the diameter difference between the capillaries was quite small; therefore, decreases in droplet size were primarily affected by the drag force triggered by the continuous-phase flow [35]. Similar to the results reported by Sugiura et al. [32] and Thorsen et al. [33], according to those reported by Umbanhowar et al., drop-size formation correlates with the interfacial tension in the two phases, in addition to capillary tip diameter and viscosity. Thus, during droplet formation, the detachment of a droplet from its capillary occurs when stream-wise forces exceed the force induced by interfacial tension [36]. Moreover, droplet size is affected by the junction geometry of the microfluidic devices, the flow rates of the continuous phase, and the physical characteristics of the fluid i.e., its interfacial tension and viscosity [37]. Furthermore, the effect of flat-tip wettability (metallic nozzle) on droplet-size formation revealed that when a droplet of liquid is applied to the wetted flat tip of the nozzle, further adhesion forces occur on the base of the droplet and affect the attachment range. Hence, the intensity of adhesion tensions in the metal phase, the dispersed phase, and the continuous phase determine the contact area of the phase fluids, which consequently affect the droplet size [38]. Schneider et al. reported a flow-focusing method in which the initial strength

of polymer concentration affected the droplets' mean particle-size distribution [39]. A high polymeric concentration caused an increase in mean particle-size distribution, which was attributed to the correlation between lower concentrations of polymer solution and lower viscosity of the dispersed phase and vice versa. Therefore, the force required by the droplet to break off from its dispersed-phase flow reduced [39]. Studies have also suggested that a lower concentration of polymeric solution in the continuous-phase flow is preferable for narrower particle dispersion. Similar results were reported by Zhu et al. regarding the formation of microspheres using a modified water-in-oil-in-water emulsion solvent-evaporation technique [40]. The effects of orifice length and width on droplet size in a flow-focusing device were investigated by Gupta et al. [41]. Their research revealed that by increasing the orifice length, the droplet size exponentially decreased until it became constant at a certain critical length and continued further beyond this length. Furthermore, by increasing the width of the orifice, a non-linear increase in droplet size occurred, and a constant orifice width resulted in the creation of a smaller-sized droplet as the capillary number increased. In their study, the effect of the capillary number on droplet size was similar to the findings reported by Wu et al. [29] and Hong et al. [30]. Regarding the connection between continuous-phase velocity and drop-formation time, the higher the velocity of the continuous-phase flow, the lower the drop-formation time [20]. Other studies highlight the effect of the continuous-phase flow (bond number, capillary number, and viscosity ratio) on droplet-break-off length, droplet-break-off time, and droplet volume [25]. Increasing the continuous-phase flow rate increased the flow's Reynolds number [22,24]. According to Sandulache et al., in one case, neither the continuous-phase flow rate nor the diameter of the external tube affected the average drop-size diameter in a jetting regime in which droplet breakage occurred some distance from the tip of the nozzle [27]. The episodic motions continuously occur provided a

relevant condition supporting the movements that can be maintained, i.e., the satisfactory concentration of the solution, the appropriate gel diameter, and a preserved temperature difference between the upper and lower walls of the enclosure. The cyclical motion of the gels within the cavity is a function of time and is determined by the sum of the external forces acting on the gels, including gravity, drag, and buoyancy. In particular, these forces are affected by variables such as solution density, gel density, drag coefficient, and gel size.

To summarize, based on the abovementioned studies and as a continuation of the previous research reported by Hasegawa et al. [13], the current study's preference is for a typical gel with a smaller contact surface (i.e., a sphere). Gels of various sizes are required to observe their behavior in an upper heating system of a rectangular cavity filled with aqueous solutions. The spherically shaped monodispersed gels were generated using a microfluidic device with a constant micro-sized nozzle (outside diameter = 300 μm) by varying the viscosity and flow rate of the continuous-phase flow. The effects of viscosity and flow-rate variations of the continuous-phase flow on gel size formation, and the volume change of the gels together with their vertically repetitive motions within the aqueous solutions were investigated.

3.2 Materials and Methods

The methodology of this research entailed a two-stage experiment. This involved generating mono-dispersed thermosensitive gels and an investigation of the swelling and shrinking behaviors of these gels within a rectangular cavity filled with a polymeric aqueous solution. Each of the sections is described as follows.

3.2.1 Method for Generating Mono-dispersed Thermosensitive Gels

In this study, NIPA gels were generated by the cross-linked polymerization of the monomer (NIPA) and N, N'-methylenebisacrylamide (BIS) as cross-linker (see Figure 5), with the aid of other three chemicals and water measured in a unit mass. The method for synthesizing the gels was similar to that described by Zhao et al. [18,19]. The chemicals included 150 mg of NIPA (Wako Chemicals, Tokyo, Japan), 5 mg of BIS (Nacalai Tesque Inc., Kyoto, Japan), 25 mg of DDBAB (Wako Chemicals) as an initiator, 10 μL of N,N,N',N'-tetramethylethylenediamine (TEMED) (Wako Chemicals) as an accelerator, 6 mg of APS (Nacalai Tesque Inc.) as an initiator, and 1.6 g of deionized water. NIPA, BIS, DDBAB, and TEMED were dissolved in half of the deionized water (0.8 g) and loaded into the first 3-mL syringe (inner diameter = 10.1 mm). Similarly, APS was dissolved in the remaining half of the deionized water (0.8 g) and loaded into the second 3-mL syringe. Two different viscosities of silicone oil (50×10^{-6} m^2/s and 300×10^{-6} m^2/s, Shin-Etsu Chemical, Tokyo, Japan) were used as continuous-phase fluids. Figure 6 shows the setup of the research apparatus. Based on the figures, the steps to synthesize the gels are described as follows: a 3mL syringe containing NIPA components and another 3 mL syringe containing APS components were precisely mounted in the linear actuator module. The tips of both syringes were closely connected to the 2mm square duct using the silicone tube, and the speed of both piston syringes was set to 0.002 mm/s. A video-recording camera was positioned close to the surface of the square duct to capture footage of the flowing gel droplets for subsequent analysis of their diameters. After inspecting all the connections, the linear actuator was activated. The actuator started pushing both piston syringes to deliver the NIPA and APS solutions at the same volumetric flow rate. Consequently, both solutions were deposited in front of the needle

nozzle prior to mixing and before forming a gel solution (considered as dispersed flow). A constant dispersed flow rate (Q_d) of 3.2×10^{-10} m^3/s was maintained throughout the study. The gel solution was then ejected from the nozzle's tip (outside diameter = 300 μ m) while the other co-flow of silicone oil (continuous-phase flow) was simultaneously ejected in the same direction by another pump (mzr-2521, HNP Mikrosysteme, Schwerin, Germany). The co-flows inside the square duct were primarily responsible for forming the gel droplets. Finally, all the gels were collected in a silicone oil reservoir on a cold plate, which was maintained at a constant temperature of -30 °C. In particular, the silicone tube within the reservoir was sufficiently long to increase the residence time of the gel droplets for the freezing process, which prevented droplet coalescence. The resulting gels were then stored in a freezer for 1 day to complete the polymerization process, and the diameter of the gel droplets flowing within the square duct was measured via image analysis. Based on the output of the diameter readings, the average diameter of the gels was calculated.

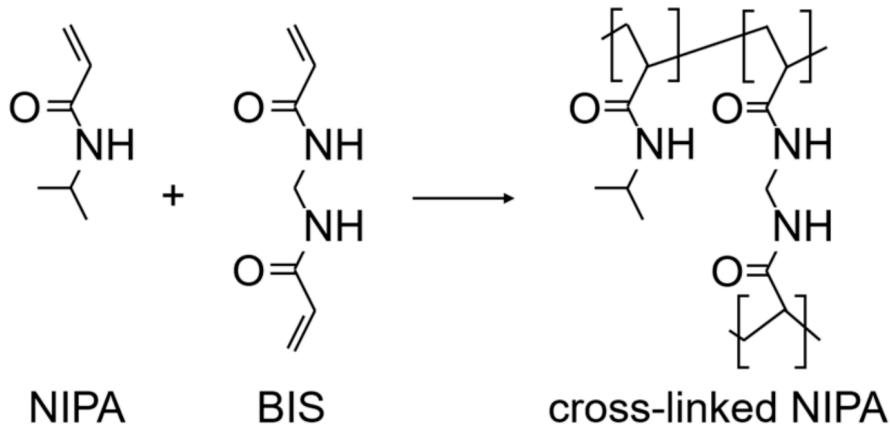

Figure 5. Synthesis of Cross-linked N-isopropyl acrylamide (NIPA) Gel

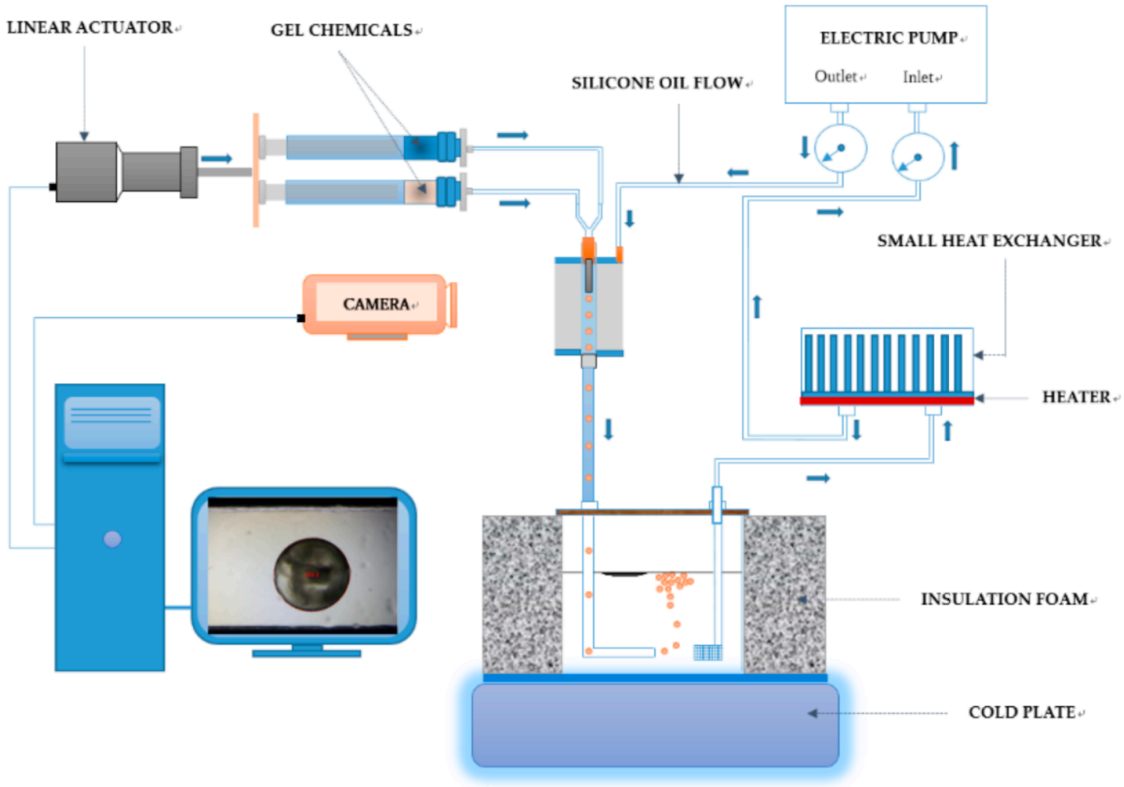

Figure 6. Schematic of Apparatus for Generating the Thermosensitive Gels

3.2.2 Method to Observe Swelling and Shrinking Behavior of Gels

In this study, the behaviors of four typical-diameter thermosensitive gels (approximately 1.3 to 0.5 mm in water at 25 °C referred to as cases A, B, C, and D, respectively) were observed in two ways. The diameter of the gels varied because of different flow rates and viscosities of the continuous-phase flows used in the formation of the droplets. First, for each case, three gel particles were selected as samples and were submerged either in deionized water or in an 11 wt % aqueous solution of sodium polyacrylate (PAANa). The concentration of the PAANa solution was fixed throughout the experiment at 11 wt % to ensure a mass density in between those of the swelling and shrinking states of the gels; this enabled the gel particles to float at 10 °C and to sink at 40 °C. The PAANa powder (average molecular weight = ~2100, Sigma-Aldrich, St. Louis, Mo, USA) and the deionized water were mixed and stirred for about 15 min to ensure a diluted solution.

During this observation, the temperature of each solution was adjusted from 5 to 40 °C in increments of 5 °C. Initially, the three gels were submerged in water, which was set to 5 °C. This condition was then maintained for 10 min before the size of the gels was recorded. Then, the water temperature was increased to 10 °C and again, after 10 min, the size of the gels was recorded. The same procedure was applied to determine the water temperature in 5 °C increments between 5 and 40 °C. After all the procedures were completed, the fluid was changed to an 11 wt % solution of PAANa. The data for this polymer solution were obtained in the same manner as that for water temperature. The recorded images were then analyzed to calculate the diameter of the three gels at different temperatures. Second, the vertical movements of the gels within the 11 wt % polymeric solution of PAANa in the cavity with temperature gradient were observed. Figure 7 shows the experimental apparatus for the observation. The primary parts of the apparatus comprised heating and cooling plates and a rectangular transparent acrylic cavity. The inner dimensions of the cavity were 16 × 16 mm (horizontal area) with a height of 13 mm. Initially, the temperatures of the hot wall (above in Figure 7) and the cold wall (below in Figure 7) of the cavity were maintained at 40 and 10 C, respectively, using water from thermostatic baths to create an upper heating system within the cavity. Eight gel particles were then inserted into the rectangular cavity, and images of their movements were captured every 20s. half (four out of eight) of the gels that exhibited active movements were then tracked in the post-processing stage.

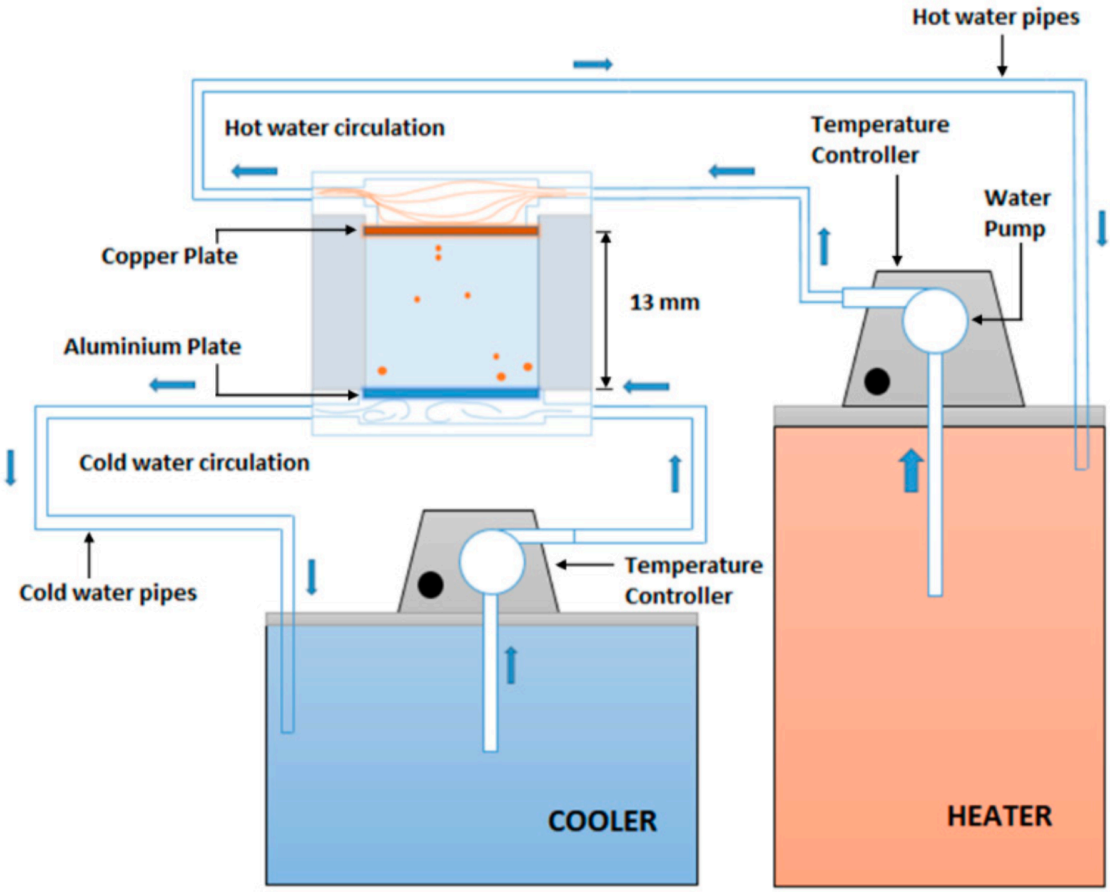

Figure 7. Schematic of the Apparatus for Mechanical Observations

3.3 Fabrication of Monodisperse Spherical Thermosensitive Gels

The initial gel formation near the tip of the needle can be seen in Figure 8a–c, which shows the droplet's growth stage, its initial necking stage, and its final separation stage. All the monodispersed droplet's growth stage, its initial necking stage, and its final separation stage. All the monodispersed thermosensitive gels used in this study were generated in the microfluidic device by setting various thermosensitive gels used in this study were generated in the microfluidic device by setting various flow rates for the silicone oil (50×10^{-6} m^2/s and 300×10^{-6} m^2/s) within a range of 3.96–15.8 $\times 10^{-9}$ m^3/s. flow rates for the silicone oil (50×10^{-6} m^2/s and 300×10^{-6} m^2/s) within a range of 3.96–15.8 $\times 10^{-9}$ m^3/s. The growth stage of the droplet was defined as the point at

which the new gel solution was ejected. The growth stage of the droplet was defined as the point at which the new gel solution was ejected from the tip of the nozzle.

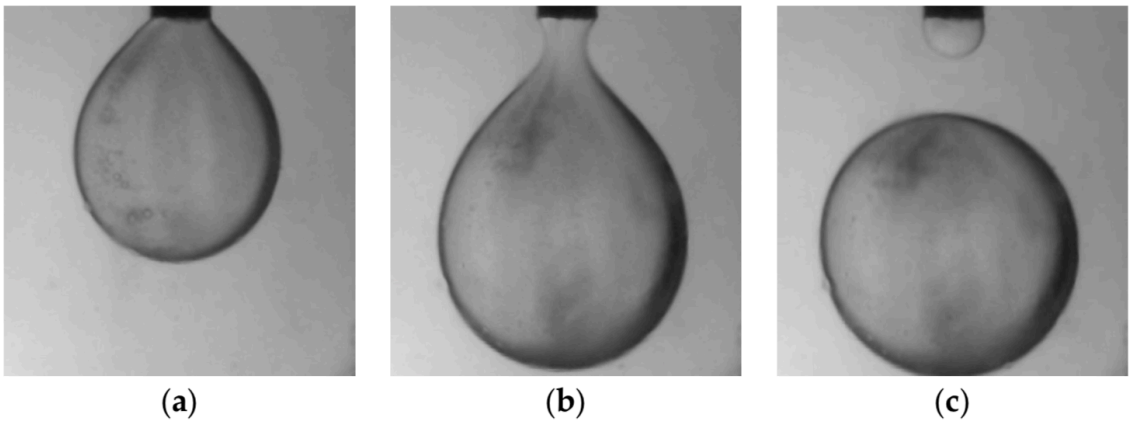

Figure 8. Images Showing a Droplet's Formation: (a) Growth Stage; (b) Necking Stage; (c) Immediately after Separation

Simultaneously, the continuous-phase flow (silicone oil) with a constant flow rate generated drag in a vertical direction (in line with gravity), which, in this case, tended to separate the developing droplet from its gel solution on the tip of the nozzle. Droplet separation could either exist in a regime or in a jetting regime. In the dripping regime, droplet breakage occurred at the tip of the nozzle (capillary tube). Meanwhile, in the jetting regime, droplet separation existed at the tip of a jet located far from the nozzle tip. In this research, droplet formation occurred in the dripping regime rather than in the jetting regime as the velocity of the inner fluid (dispersed phase) was slower than that of the continuous-phase fluid [27]. Hence, the condition supported the breakage of droplets (separation), which occurred near the tip of the nozzle as shown in Figure 8. When the continuous-phase flow rate was gradually increased from 5.94×10^{-9} m^3/s to 15.8×10^{-9} m^3/s (for the both values of viscosity), the diameter of the gel droplets visibly decreased (as shown in Figure 5a with the reference letters (A–D). The relationship between an increasing continuous-phase flow rate and the average droplet diameters for

the both viscosities (50×10^{-6} m^2/s and 300×10^{-6} m^2/s) are shown in Table 1.

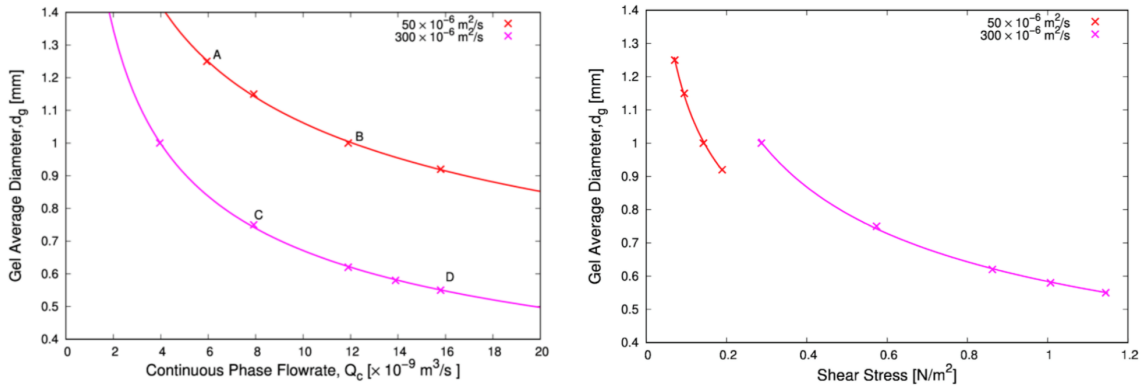

(**a**) (**b**)

Figure 9. Relationship between (a) The Continuous-phase Flow Rate and The Gel-droplets' Average Diameter, (b) The Shear Stress and The Average Diameter with Respect to Silicone Oil Viscosity

Table 1. Average gel-droplet diameter for the two types of continuous-phase flows.

Flow Rate of 50×10^{-6} m^2/s ($\times 10^{-9}$ m^3/s)	Gel Diameter (mm)	Flow Rate of 300×10^{-6} m^2/s ($\times 10^{-9}$ m^3/s)	Gel Diameter (mm)
5.94	1.29	3.96	1.04
7.92	1.19	7.92	0.77
11.9	1.04	11.9	0.65
15.8	0.95	13.9	0.60
		15.8	0.57

A correlation was evident between the diameter of the generated droplet (d_g) and the flow rate of the continuous-phase flow (Q_c) for each of the silicone oils' viscosities, which can be expressed as follows:

$$d_g = 2.2 Q_c^{-0.32} \text{ for } 50 \times 10^{-6} \text{m}^2\text{/s silicone oil (1),}$$

and

$$d_g = 1.8 Q_c^{-0.43} \text{ for } 300 \times 10^{-6} \text{ m}^2\text{/s silicone oil. (2)}$$

The correlations indicate that the flow rate of the continuous phase significantly affected

the diameter of the generated droplets. The two curved lines shown in Figure 9a define the correlation between the continuous-phase flow rate and the average diameter of the droplets with respect to the two kinematic viscosity values of 50×10^{-6} m^2/s and 300×10^{-6} m^2/s. During the experiment, gel particles were prepared in nine cases by varying the continuous-phase flow rate and the kinematic viscosity. The coefficient of variations, the ratio of standard deviation, and the average value of the droplets' diameter calculated from hundreds of droplets for all the nine cases were <10%; therefore, droplet formation was considered to be monodispersed [25]. From the graph, it is apparent that the diameter of the droplets decreased as the continuous-phase flow rate increased; the same trend was evident for both kinematic viscosity values. In particular, the 50×10^{-6} m^2/s silicone oil could generate larger gel diameters than the 300×10^{-6} m^2/s silicone oil at the same continuous-phase flow rate values. A key result of these results is that a higher-viscosity continuous-phase flow (300×10^{-6} m^2/s) can generate smaller gel droplets than a lower viscosity flow (50×10^{-6} m^2/s) or, more generally, the smaller the kinematic viscosity of the continuous-phase flow rate, the bigger the droplet diameter that can be generated. Moreover, this results was supported by the results of other researchers [24,38,42-44]. To illustrate this using one of the nine cases as an example, $7.92\ x\ 10^{-9}\ m^3/s$ of the $50\ x\ 10^{-6}\ m^2/s$ silicone oil generated a gel droplet of 1.19 mm in diameter. However, for the $300\ x\ 10^{-6}\ m^2/s$ silicone oil with an identical flowrate, the diameter of the gel droplet was only 0.77 mm, i.e., the gel droplet decreased in volume by 72%. This significant decrease in droplet`s volume was clearly affected by an increasing flow rate and the kinematic viscosity of the continuous-phase flow. The increase in the continuous-phase flow rate correlated with an increase in drug induced by the flow, which supported droplet detachment from the tip of the nozzle. Hence, a smaller size of droplet was

generated as the droplet-formation time was decreased. Furthermore, an increase in viscosity of the continuous-phase flow contributed to an increase in drag force. According to Scheele et al., a greater drag force correlate with the diameter of the detached droplet [34].

Therefore, this study determined that droplet size was mostly affected by flowrate and the kinematics viscosity of the continuous-phase fluid (silicone oil). To examine the effect of these two factors on the droplet size, we estimate the shear stress on the interfaces as $\mu u_C/\delta$ where the average velocity u_C was continuous phase flow rate Q_C divided by the duct cross section (4 mm^2), neglecting the needle cross section which was less than 2% of the duct's one. The reference length δ was taken as half of the duct width. The dynamic viscosity μ was calculated using densities of 958 and 966 kg/m^3 for 50×10^{-6} m^2/s and 300×10^{-6} m^2/s silicone oil respectively. The results are shown in Figure 9b. The two curves show a unified trend through the whole range of the shear stress, although there exists a discontinuity between them. It is presumably due to the difficulty to accurately evaluate the shear rate since the flow pattern was not simple around the droplet evolving near the nozzle tip in a narrow duct which width was comparable to the droplet size.

3.4 Swelling and Shrinking Phenomena of Thermosensitive Gels in Constant Temperature Field

Figure 10 shows images of the selected gels submerged in water at temperatures of 10, 25, 40°C for cases A and C and shows their physical appearance after polymerization. Three gel samples were selected and placed on an acrylic plate for observation. A similar shrinkage trend was exhibited by a cylindrical NIPA gel reported by Hasegawa et al. [13]. The size of the gel rod significantly decreased when the temperature of the solution was increased from 10 to 40°C. At 40°C, the NIPA gel shrank and demonstrated a negative

thermal expansion characteristic.

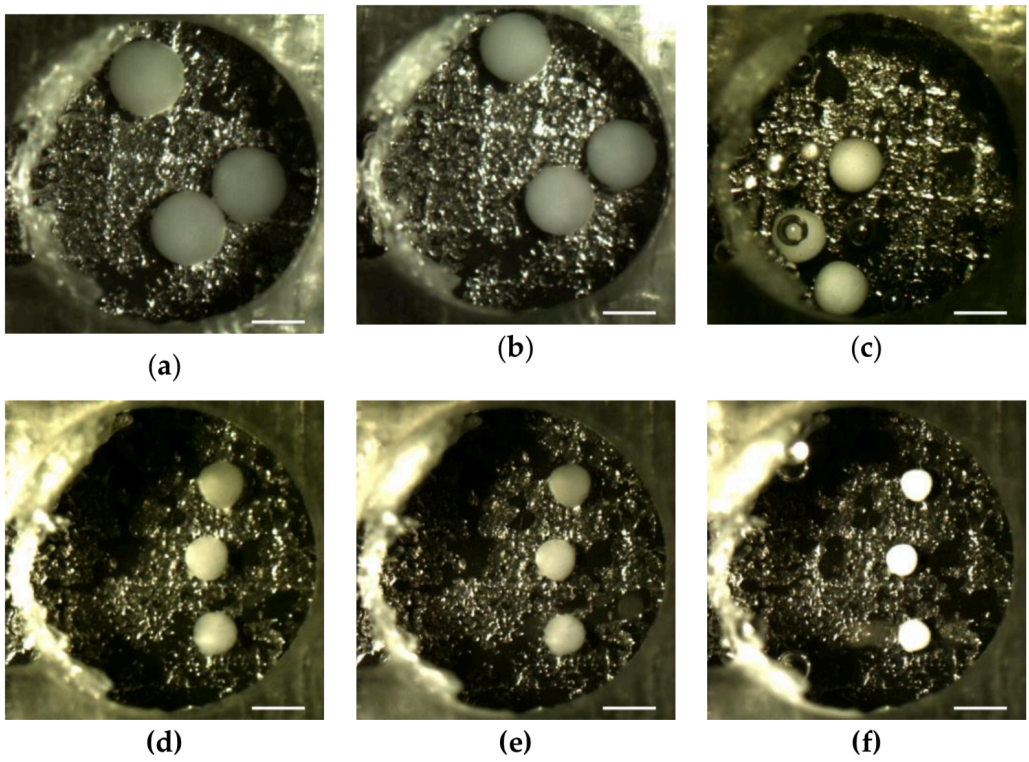

Figure 10. Gel Particles Submerged in Water at Elevated Temperatures: (a) 50 C; (b) 25 C; (c) 40 C in Case A and (d) 10 C; (e) 25 C; (f) 40 C in Case C (The Scale Bar Corresponds to 1mm)

Figure 11 shows the variation in gel diameter for case A, B, C, and D in water at different temperatures. Figure 12 shows the variations in gel diameter with the PAANa solution for the same-sized gels. Both figures show that as the temperature of the aqueous solution increased, the diameter of the gels oppositely decreased. This general correlation

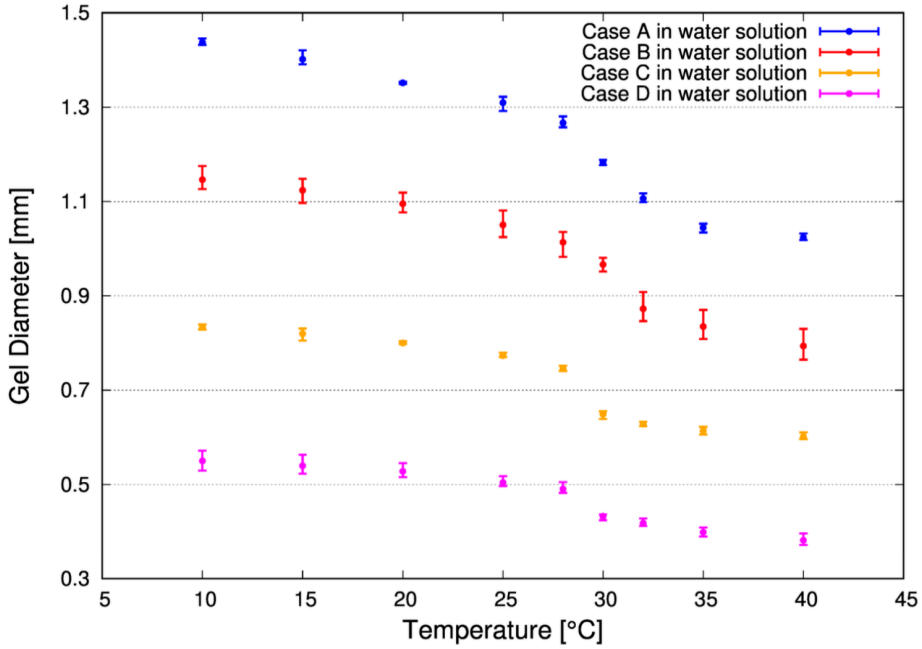

Figure 11. Variations in Gel Diameter at Elevated Temperatures in the Water Solution

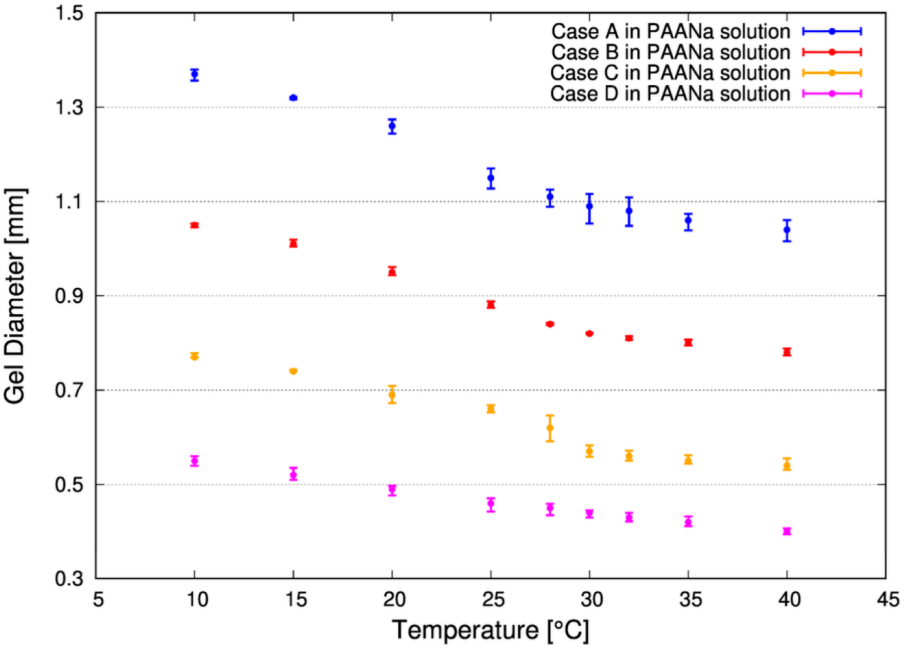

Figure 12. Variations in Gel Diameter at Elevated Temperatures in The Sodium Poly-acrylate (PAANa) Solution

is an evident for both solution types (water and PAANa solution). Indeed, the exact pattern of both figures was different, especially within the range of 25-30°C, where the most significant volume change occurred. For case A in both figures, considerable changes in gel diameter occurred at temperatures between 25 and 35°C. For the smaller-

sized gels, as shown in case C and D, it is clear that the gels' average diameters slightly decreased as the water temperature increased. Moreover, case A and B (which represent a bigger gel size) showed a significant decrease in diameter at temperatures between 25 and 35°C as the temperature of the polymer solution increased. The vertical error bars shown in the plotted curves of the figures indicate a range of the three measured values.

The plots reveal a slight decrease in gel diameter within two temperature ranges of the polymeric solution: 10-25°C and 35-40°C. However, in the temperature ranges between 25 and 35°C, a sharp decrease in gel size is an evident because significant changes in gel volume occurred within this range.

As shown in both graphs, a significant difference in the slope of the curve is observed at a temperature range between 25 and 30°C. In this range, the gels exhibited a sharper response to the increasing temperature than that of the other two ranges. In particular, the largest slope is an evident at temperature between 25 and 30°C. This phenomenon is attributed to the particular characteristics of the NIPA gel used in the experiment. At lower temperatures, the gels were in a swollen state and were larger in size. However, at higher temperatures, the gels shrank and became smaller as water molecules detached from the polymer chain (hydrophobic state). Water-molecule detachment started on the outer layer of the gels and continued to the inner layers. The plotted points represent the average value of the three gel samples, and the curve was obtained by polynomial (quaternary) approximation. The error bars in the figure represent the deviation in measured value at each temperature. The graph reveals that the diameter of the gel particles gradually decreased as the temperature of the polymer solution increased, indicating a negative thermal expansion characteristic. When the temperature of the solution was constantly modified at specific intervals, the gels showed reversible transformation from a swelling state to a shrinking state before reverting to their initial

state. Furthermore, the polymeric gel's higher molecular weight had a longer chain length and possessed a network with a lower cross-link density, which resulted in higher swelling rates in the gel [42].

The volumetric change in the gel particle is discussed below. A gel particle was approximated to a sphere of diameter d_g such that its volume V_g was estimated as $\pi\, {d_g}^3/6$. The relationship between V_g and the temperature of the gels in the aqueous solution T together with the relationship between the gels' volume ratio V_g/V_{shrink} and T can be seen in Figure 13 and Figure 14 where V_{shrink} is the volume at 40°C. Figure 13 clearly demonstrate that case A, which is represented by the blue line, had the biggest gel volume, followed by case B, C, and D. Figure 14 shows that the biggest change in gel volume occurred between 25 and 30 °C. As in Figure 13, the smallest gel (case D) showed no significant volume changes in the same range of temperature. Thus, by considering the volume ratio of gel V_g/V_{shrink}, the temperatures at which significant volume changes occurred could be clearly observed. Interestingly, as shown in Figure 14, all sizes of gel exhibited similar volume ratio patterns when the temperature of the aqueous solution increased.

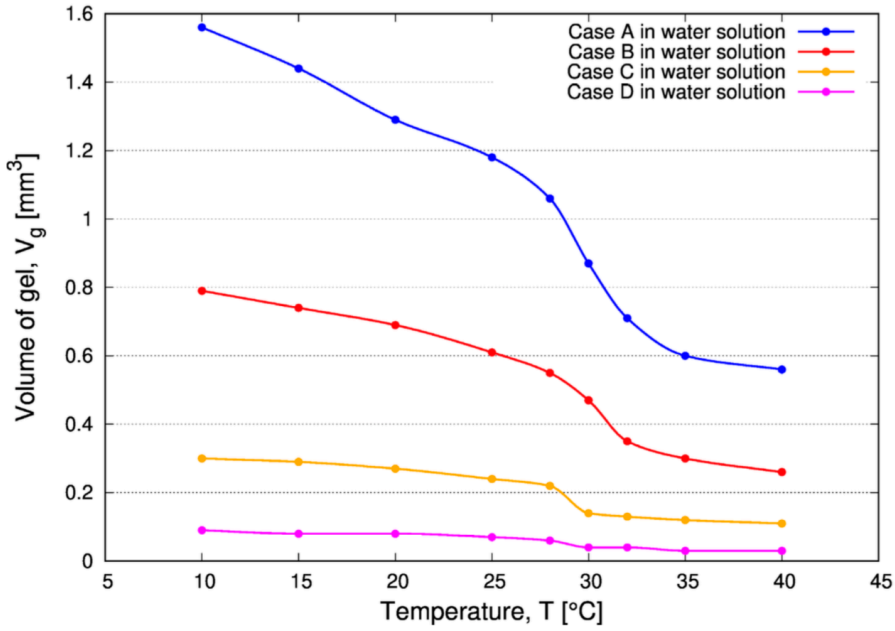

Figure 13. Variations in Gel Volume at Elevated Temperatures in The PAANa Solution

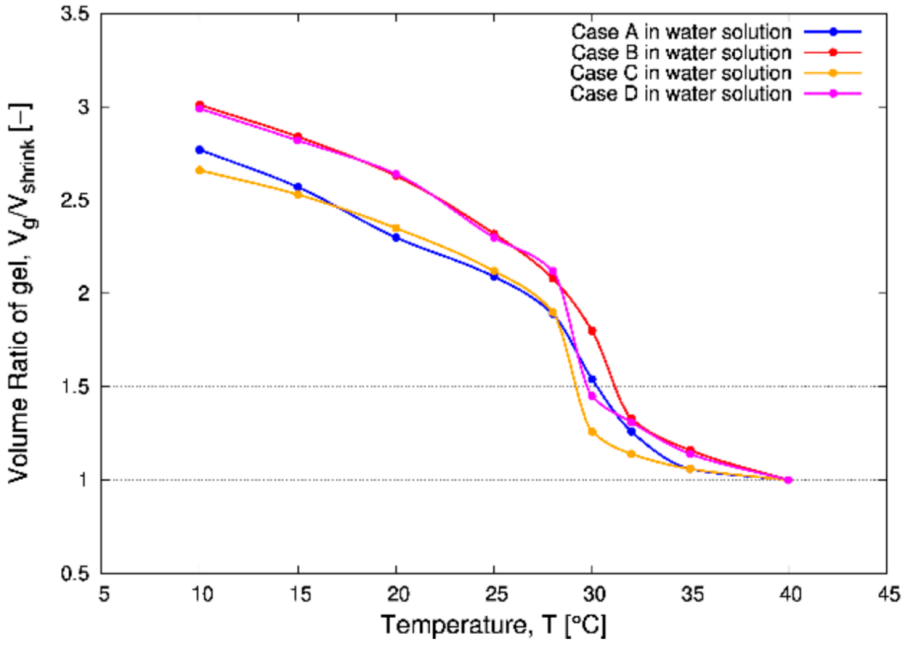

Figure 14. Variations in Gel Volume Ratio at Elevated Temperatures in The PAANa Solution

Figure 13 clearly demonstrate that case A, which is represented by the blue line, had the biggest gel volume, followed by case B, C, and D. Figure 14 shows that the biggest change in gel volume occurred between 25 and 30 °C. As in Figure 13, the smallest gel

(case D) showed no significant volume changes in the same range of temperature. Thus, by considering the volume ratio of gel V_g/V_{shrink}, the temperatures at which significant volume changes occurred could be clearly observed. Interestingly, as shown in Figure 14, all sizes of gel exhibited similar volume ratio patterns when the temperature of the aqueous solution increased.

However, the variation in ratios occurred in quite a small range between 2.7 and 3.0 at 10 °C. Moreover, a significant volume change occurred between 25 and 35 °C. It is evident from both figures that the largest volume change probably occurred at about 30 °C. Figure 15 shows the correlation between gel volume and the temperature of the PAANa solution. For the PAANa solution, similar patterns of V_g–T showed by the all gel sizes were evident, as shown in the figure. As the temperature of the PAANa solution increased from 10 to 40 °C, the volume of the gels in all cases inversely decreased.

Figure 16 shows the relationship between the volume ratio and the temperature of the PAANa solution. The swelling volumes in the solution were lesser compared with those in water, while the volumes in a shrunken state at 40 °C were almost same as those in water, resulting in V_g/V_{shrink} values between 2.3 and 2.9. Note that the volume ratio of gels in the PAANa solution slowly decreased for the entire range as the temperature of the solution increased. This is in contrast to water for which the volume ratio significantly decreased between 25 and 35 °C, and the ratios remained almost constant at temperatures above this range. These differences in the two fluids are clearly illustrated in Figure 17 and Figure 18, where only cases A and D were selected as examples.

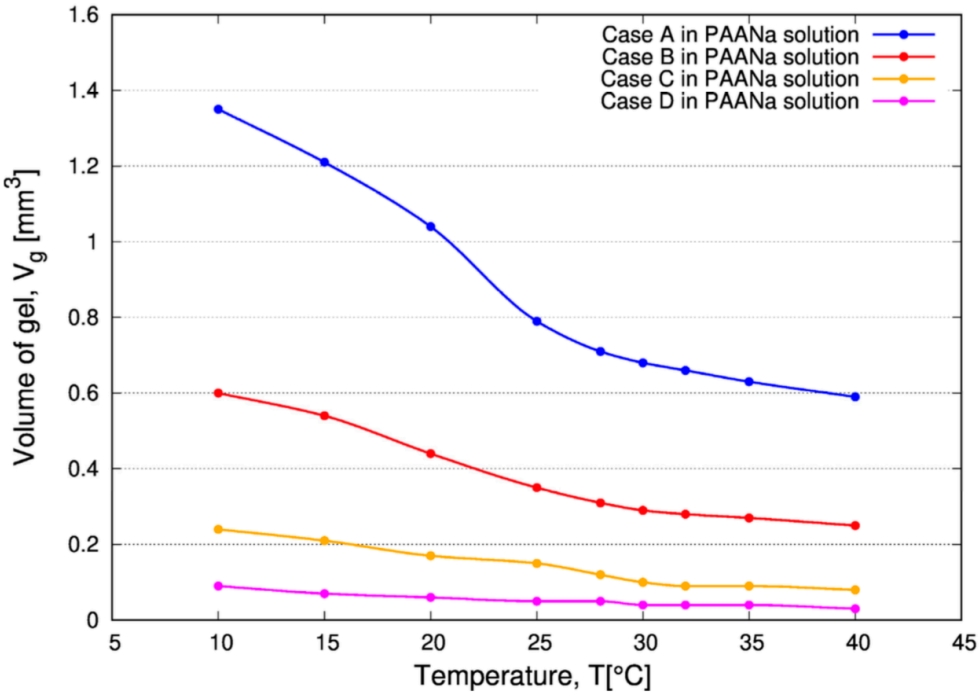

Figure 15. Variations in Gel Volume at Elevated Temperatures in the PAANa Solution

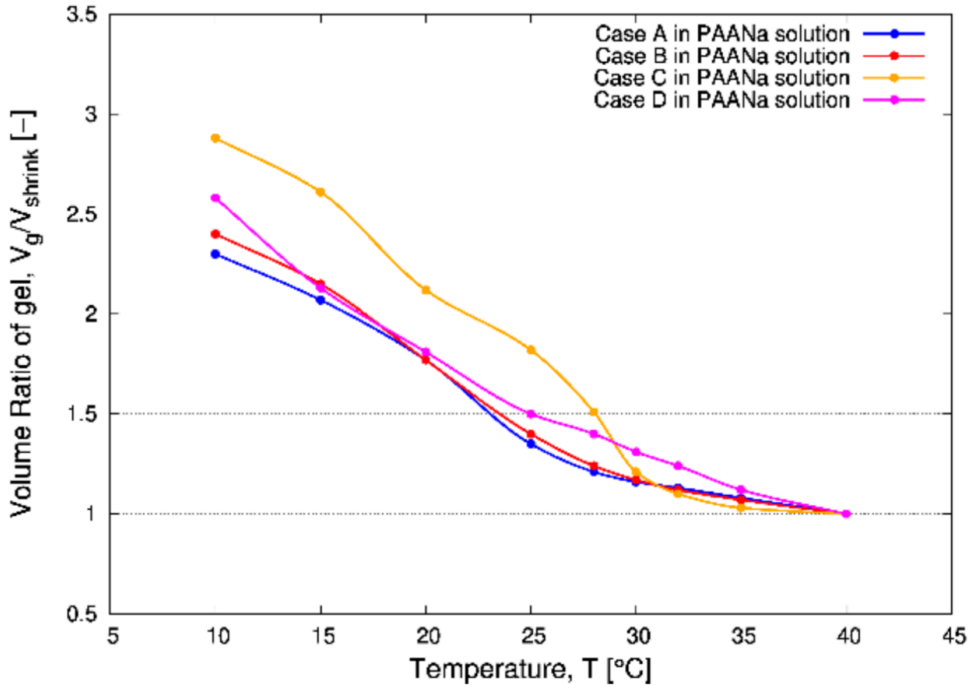

Figure 16. Variations in Gel Volume Ratio at Elevated Temperatures in The PAANa Solution

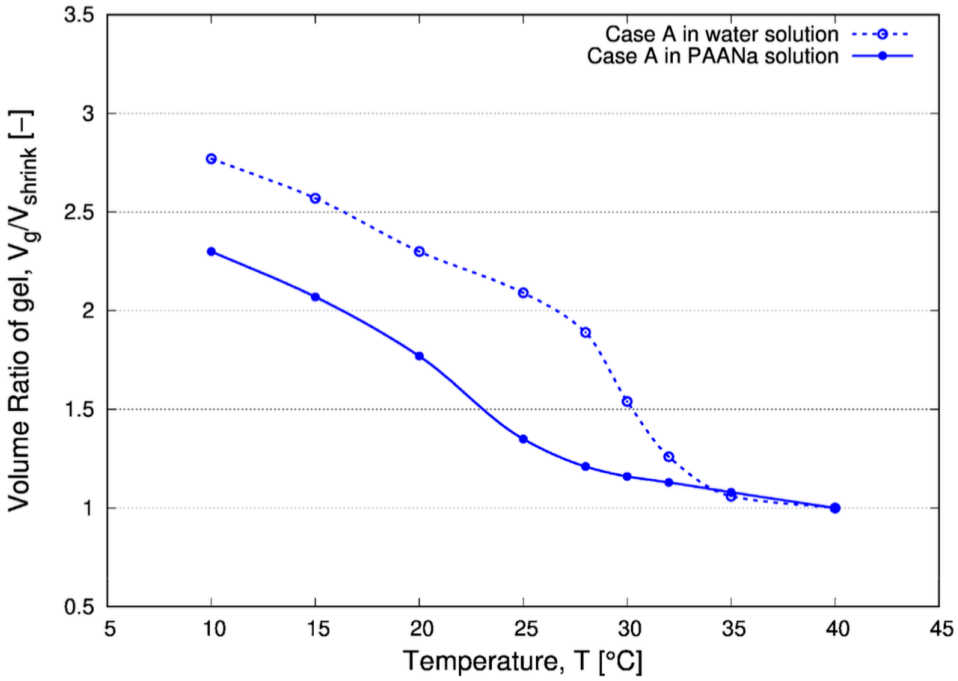

Figure 17. Comparison of The Gels' Volume Ratio in Water and in PAANa Solution for Case A

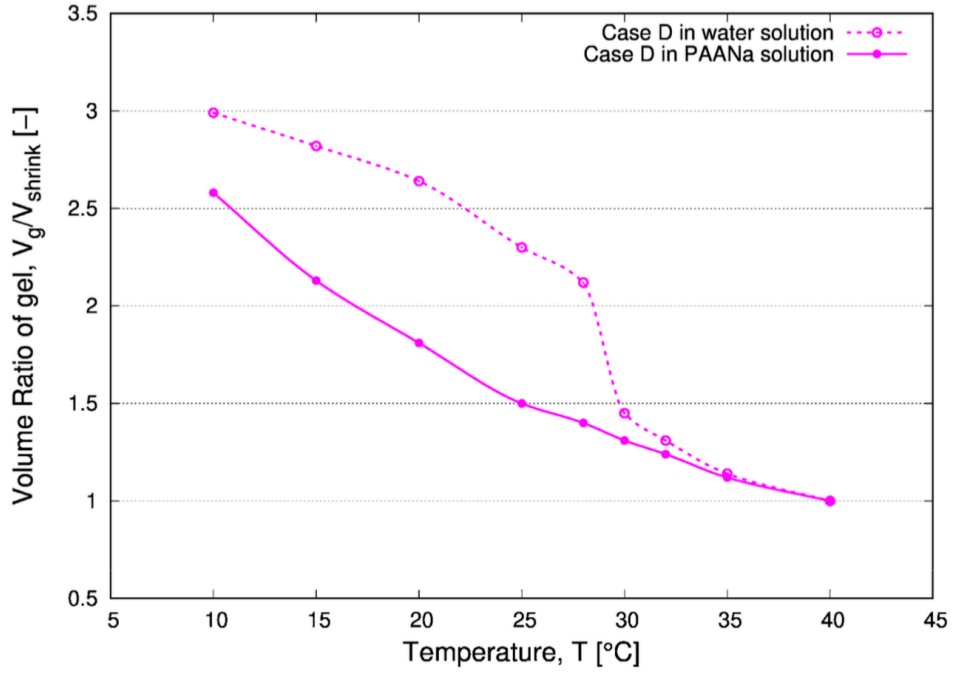

Figure 18. Comparison of The Gels' Volume Ratio in Water and in The PAANa Solution for Case B

3.5 Dynamical Behavior of Thermosensitive Gels in Aqueous Polymeric Solution with Temperature Gradient

Figure 19 shows the periodic movements of the gels within the rectangular cavity. The trajectories of the particles in circles are shown in Figure 20 with the corresponding colors. Eight gels were used in the experiment, and four active gels were selected for path tracking. The four gels can be identified by different colors (green, blue, red, and violet), which correspond to the curves in the following charts. The figures run in sequence from the top left image, where all the gels were still at the bottom of the rectangular cavity, to the images on the right. Similar sequences were applied to the images in the second, third, and fourth rows. The gels were seen to be moving in vertical up-and-down cyclical patterns. Figure 20 shows the repetitive up-and-down movements of the gels within the PAANa solution for case A. The figure confirms that the gels moved vertically several times for a period of approximately 10 minutes before gradually damped in respect of time. The gels' movements were affected by the forces of buoyance, drag, and gravity, which acted on the gels in the solution. At the start of experiment, the swollen state gels were inserted into the polymer solution at 2mm from the bottom of the cavity. The gels moved upward (because their density was lower than that of the polymer solution) until they reached a higher position 12 mm from the bottom of the cavity. In this position, the gels absorbed heat from the cavity's upper wall and transitioned to a state of shrinkage. Under this condition, the gels' densities increased above that of the polymer solution before moving downward for the first time until they were 1 mm from the bottom of the cavity. The lower temperature at the bottom caused the gels to transition to a swollen state. Moreover, buoyance was higher in this position, which forced the gels upward until they reached the second-top position at 12 mm from the bottom of the cavity.

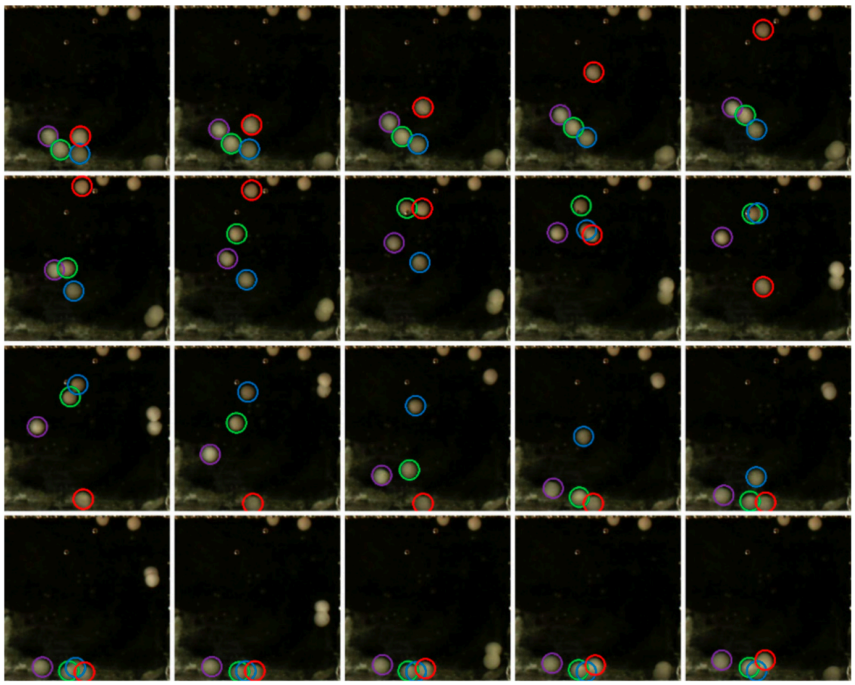

Figure 19. The Periodic Movement of Gels (Case A) in The PAANa Solution from 28-40.67 Minutes after The Start in Increments of 40 Seconds

The top position of the gels gradually decreased over time. Two of the gels reached their equilibrium conditions earlier than the third gel; they then stopped moving between 4 and 4.5 mm from the bottom of the cavity. Evidently, at 170 minutes, the amplitude of gel 1 was considerably reduced because of collision and adhesion with gel 3, which caused a counteraction of their movements. The gels eventually broke up, and gel 1 started moving again; however, all the gels stopped moving at 250 minutes.

Figure 21 shows the gel movements of case B. Although the amplitude of the vertical motion was small compared with case A, the gels exhibited similar movements for a period of 10 min followed by a gradual decrease in amplitude. At the start of the experiment for case B, some gels became stuck to the heat transfer surfaces (gels 1 and 4 were on top, and gel 3 was on the bottom). Gels 1 and 2 became affixed to other gels (whose trajectories are not shown) at 100 and 120 min, respectively, and could no longer

be tracked. At 140 min, gel 4 became stuck to six other gels to form a cluster of seven. Gel 3 was the only gel that individually moved until the end of the experiment.

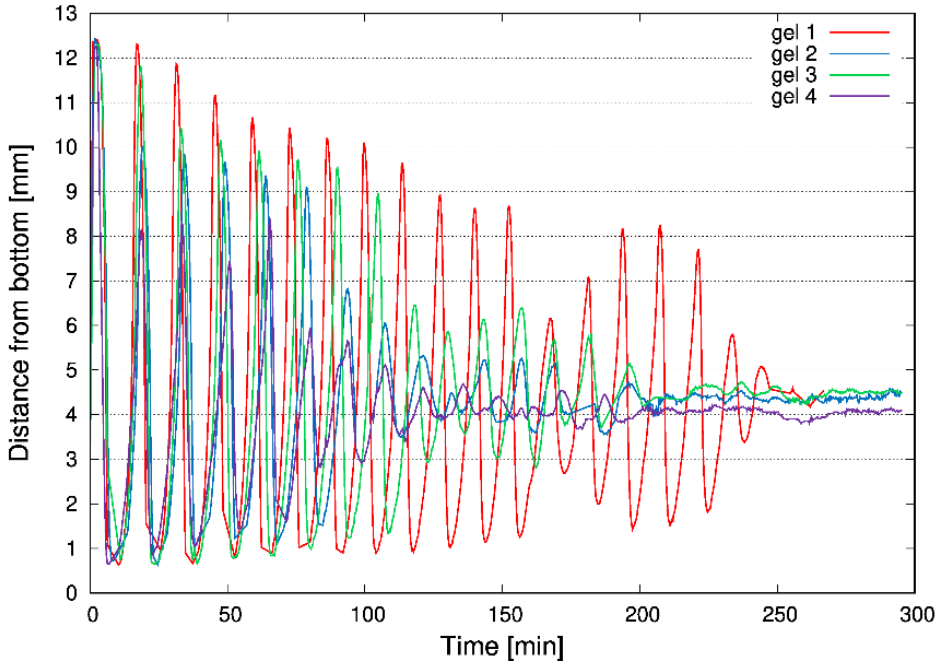

Figure 20. Vertical Movements of Case A Gels in The PAANa Solution

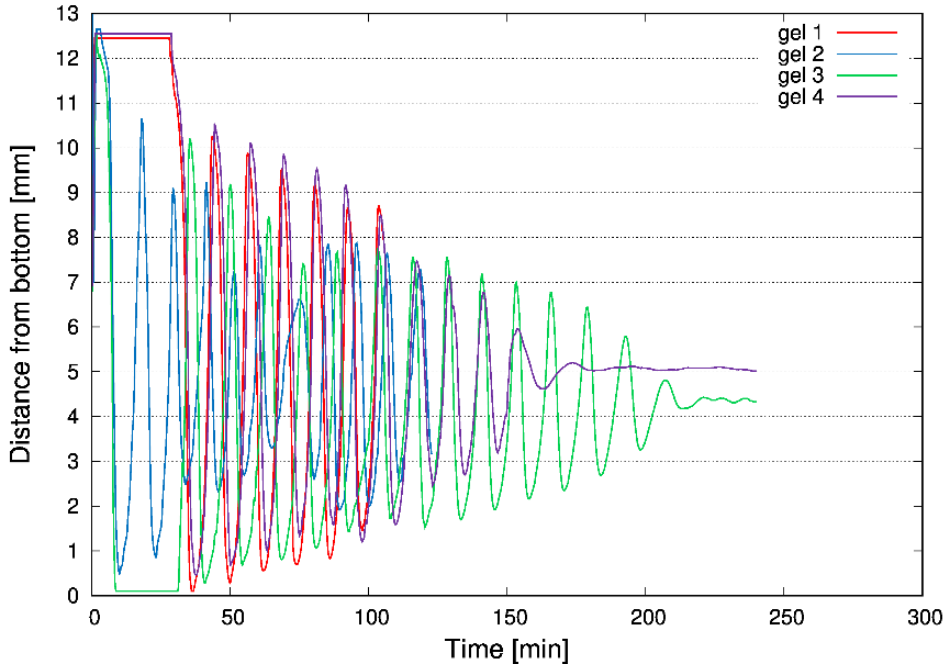

Figure 21. Vertical Movements of Case B in The PAANa Solution

Figure 22 shows the results of case C. At the start, gel 1 was positioned at approximately 5 mm from the bottom of the cavity in a state of shrinkage. It then started to move downward until it reached a position at 2 mm above the base of the cavity. At this level, the gel was affected by the lower temperature of the cooling source, and it started to swell; a quantity of the surrounding fluid entered the gel's structure, and its diameter slowly increased. The gels's density became lower than that of the surrounding PAANa solution, and it started to gradually move upward until it reached a position at 3.5 mm above the base of the cavity. In this position, the gel started to shrink again because of the higher temperature of the surrounding fluid. A specific amount of aqueous polymer solution was squeezed out of the gel's structure, and its density became higher than that of the solution. Consequently, the gel moved downward again until it reached a position 3mm above the base of the cavity. Over time, only very small fluctuations in position were observed, and the gel became stagnant at 2.8 mm above the base of the cavity. In this case, the up-down movement was only seen during approximately the first 20 minutes. Similar patterns of small initial amplitudes and short continuations of up-down movements were observed for case D, as shown in Figure 23. There is a difference in the oscillation modes of the gels in case B and C, which could not be clarified in this study. However, the up-and-down movement continued until the gels and their surrounding fluids reached a state of equilibrium, at which point the gravitational force and buoyancy force exerted on the gels canceled each other out. This occurred more quickly for the smaller gel and is qualitatively reasonable because the smaller gels could achieve relatively quicker heat and mass transfer with their surrounding fluids.

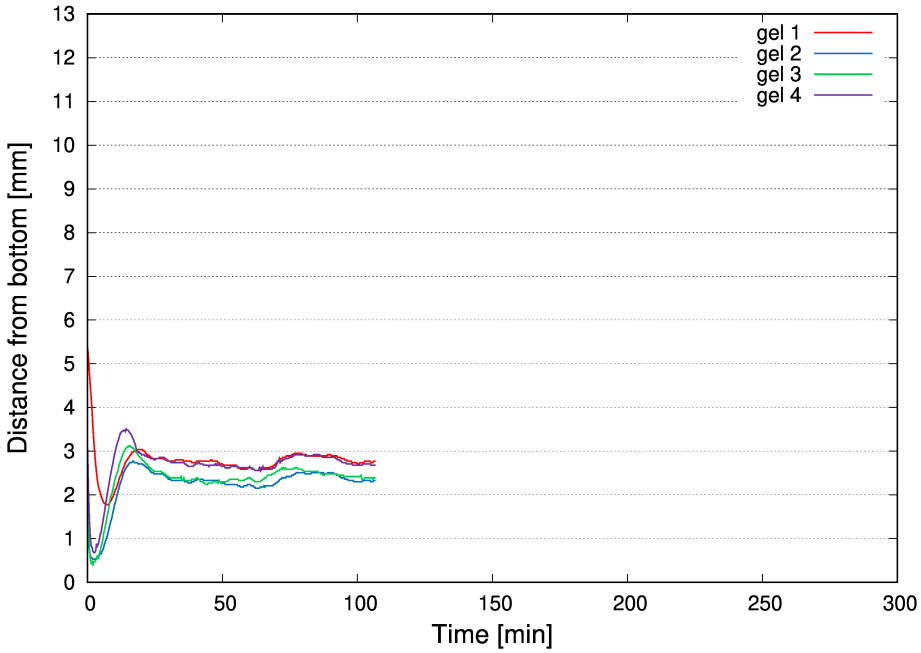

Figure 22. Vertical Movements for Case C in The PAANa Solution

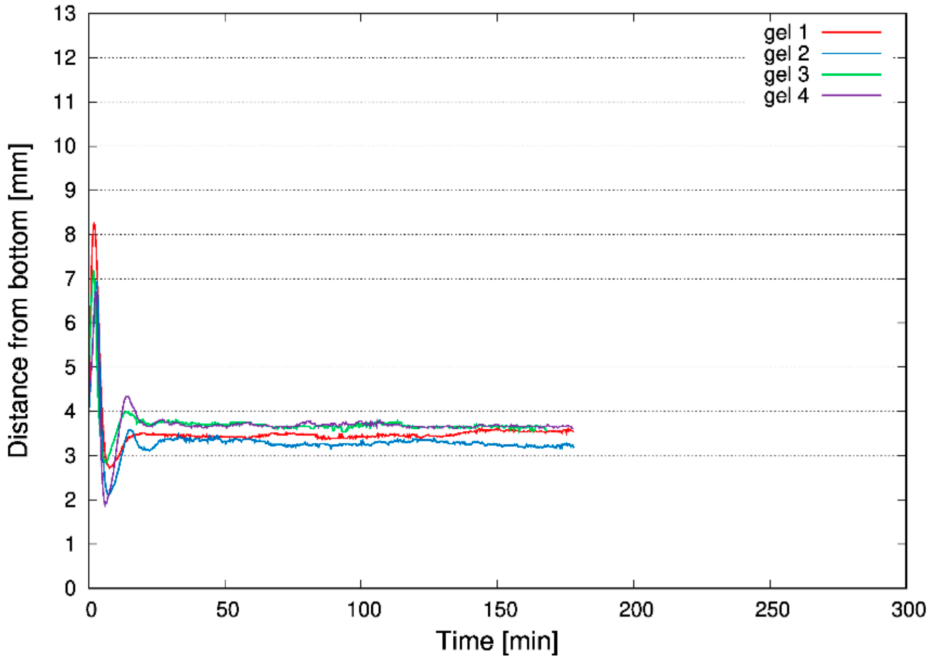

Figure 23. Vertical Movements for Case D in The PAANa Solution

3.6 Conclusions

When producing spherical gel particles, diameter of the gel droplets can be controlled by adjusting the continuous-phase flow rate and the kinematic viscosity. Both shrinking and swelling of the gels occurred after polymerization because of changes in the ambient temperature of the polymeric solution, which resulted in negative thermal expansion. The gel particles required a certain length of time to thoroughly respond to the temperature changes of the PAANa polymeric solution both swollen and shrunken states. In fact, more than 10 minutes were required for the gels to swell and shrink to their steady-state particle size. This phenomenon affected the floating behavior of the gel particles in the polymeric aqueous solution. When the temperature of the polymeric solution was 40°C, the density of the gel particles was greater than tat of the surrounding polymeric solution; moreover, the gel particles tended to settle because the acting gravitational force was greater than the buoyance force. However, when the temperature was adjusted to 10°C, the gel particle's densities were lower than that of the aqueous solution. Furthermore, because buoyance force exceeded gravitational force, the particles tended to float. The gels with larger diameters tended to have longer vertical periodic movements and required more time to reach their equilibrium state compared to gels with smaller diameter.

Acknowledgements: This research was funded by JPS KAKENHI, grant number JP17K06191, and the Indonesia Endowment Fund for Education (LPDP) in providing funding via a BUDI-LN Scholarship Scheme.

References

1. Matanovic, M.R.; Kristl, J.; Grabnar, P.A. Thermoresponsive polymers: Insight into decisive hydrogel characteristics, mechanisms of gelation, and promising biomedical applications. *Int. J. Pharm.* **2014**, *472*, 262–275.
2. Ganorkar, C.R.; Liu, F.; Baudy, M.; Kim, S.W. Modulating insulin-release profile from pH/ thermosensitive polymeric beads through polymer molecular weight. *J. Control. Release* **1999**, *59*, 287–298.
3. Hoffman, A.S. Intelligent polymers in medicine and bio-technology. *Artif. Organs* **1995**, *19*, 458–467.
4. Ding, Z.; Fong, R.B.; Long, C.J.; Stayton, P.S.; Hoffman, A.S. Size-dependent control of the binding of biotinylated proteins to streptavidin using a polymer shield. *Nature* **2001**, *411*, 59–62.
5. Jeong, B.; Kim, S.W.; Bae, Y.H. Thermosensitive sol-gel reversible hydrogels. Advance Drug Delivery Reviews. **2002**, *54*, 37–51.
6. Klouda, L. Thermoresponsive hydrogels in biomedical applications: A seven-year update. *Eur. J. Pharm. Biopharm.* **2015**, *97*, 338–349.
7. Ward, M.A.; Georgiou, T.K. Thermoresponsive polymers for biomedical applications. *Polymer* **2011**, *3*, 1215–1242.
8. Boustta, M.; Colombo, P.E.; Lenglet, S.; Poujol, S.; Vert, M. Versatile UCST-based thermoresponsive hydrogels for loco-regional sustained drug delivery. *J. Control. Release* **2014**, *174*, 1–6.
9. Iizawa, T.; Taketa, H.; Maruta, M.; Ishido, T.; Gotoh, T.; Sakohara, S. Synthesis of porous poly (N-isopropylacrylamide) gels beads by sedimentation polymerization and their morphology. *J. Appl. Polym. Sci.* **2007**, *104*, 842–850.

10. Sisworo, R.R.; Hasegawa, M.; Kawabata, N. Convective heat transfer inside a fluid-filled rectangular cavity. *Int. J. Appl. Eng. Res.* **2018**, *13*, 1789–1797.
11. Wang, H.D.; Chu, L.Y.; Yu, X.Q.; Xie, R.; Yang, M.; Xu, D.; Zhang, J.; Hu, L. Thermosensitive affinity behavior of poly(N-isopropylacrylamide) hydrogels with β-cyclodextrin moieties. *Ind. Eng. Chem. Res.* **2007**, *46*, 1511–1518.
12. Zhang, N.; Zheng, S.; Pan, Z.; Liu, Z. Phase transition effects on mechanical properties of NIPA hydrogel. *Polymers* **2018**, *10*, 1–11.
13. Hasegawa, M.; Kamikido, T.; Kawabata, N. Behavior of thermo-sensitive gel in polymer solution. *Int. Commun. Heat Mass Transf.* **2016**, *76*, 55–58.
14. Oh, K.S.; Oh, J.S.; Choi, H.S.; Bae, C.Y. Effect of cross-linking density on swelling behavior of NIPA gel particles. *Macromolecules* **1998**, *31*, 7328–7335.
15. Li, Y.; Tanaka, T. Study of the universality class of the gel network system. Journal of Chemical Physics. **1989**, *90*, 5161.
16. Zhang, X.Z.; Zhuo, R.X. Preparation of fast responsive, temperature-sensitive poly (*N*-isopropylacrylamide) hydrogel. *Macromol. Chem. Phys.* **1999**, *200*, 2602–2605.
17. Zhang, X.Z.; Zhuo, R.X.; Yang, Y. Using mixed solvent to synthesize temperature sensitive poly(*N*-isopropylacrylamide) gel with rapid dynamics properties. *Biomaterials* **2002**, *23*, 1313–1318.
18. Zhao, Q.; Sun, J.; Zhou, Q. Synthesis of macroporous poly (*N*-isopropylacrylamide) hydrogel with ultrarapid swelling-deswelling properties. *J. Appl. Polym. Sci.* **2007**, *104*, 4080–4087.
19. Zhao, Q.; Sun, J.; Ling, Q.; Zhou, Q. Synthesis of macroporous thermosensitive hydrogels: A novel method of controlling pore size. *Langmuir* **2009**, *25*, 3249–3254.

20. Bouquey, M.; Serra, C.; Berton, N.; Prat, L.; Hadziioannou, G. Microfluidic synthesis and assembly of reactive polymer beads to form new structured polymer materials. *Chem. Eng. J.* **2008**, *135*, S93–S98.
21. Seo, M.; Nie, Z.; Xu, S.; Mok, M.; Lewis, P.C.; Graham, R.; Kumacheva, E. Continuous microfluidic reactors for polymer particles. *Langmuir* **2005**, *21*, 11614–11622.
22. Nisisako, T.; Torii, T.; Higuchi, T. Novel microreactors for functional polymer beads. *Chem. Eng. J.* **2004**, *101*, 23–29.
23. Zygan, Z.T.; Cabral, J.T.; Beers, K.L.; Amis, E.J. Microfluidic platform for the generation of organic-phase microreactors. *Langmuir* **2005**, *21*, 3629–3634.
24. Quevedo, E.; Steinbacher, J.; McQuade, D.T. Interfacial polymerization within a simplified microfluidic device: Capturing capsules. *J. Am. Chem. Soc.* **2005**, *127*, 10498–10499.
25. Cramer, C.; Fischer, P.; Windhab, E.J. Drop formation in a co-flowing ambient fluid. *Chem. Eng. Sci.* **2004**, *59*, 3045–3058.
26. Zhang, D.F.; Stone, H.A. Drop formation in viscous flows at a vertical capillary tube. *Phys. Fluids* **1997**, *9*, 2234–2242.
27. Sandulache, M.; Paullier, P.; Bouzerar, R.; Yzet, T.; Baledent, O.; Salsac, A. Liquid injection in confined co-flow: Application to portal vein embolization by glue injection. *Phys. Fluids* **2012**, *24*, 081902.
28. Lan, W.; Jing, S.; Guoa, X.; Li, S. Study on "interface—shrinkage—driven" breakup of droplets in co-flowing microfluidic devices. *Chem. Eng. Sci.* **2017**, *158*, 58–63.
29. Wu, P.; Luo, Z.; Liu, Z.; Li, Z.; Chen, C.; Feng, L.; He, L. Drag-induced breakup mechanism for droplet generation in dripping within flow focusing microfluidics. *Chin. J. Chem. Eng.* **2015**, *23*, 7–14.

30. Hong, Y.; Wang, F. Flow rate effect on droplet control in a co-flowing microfluidic device. *Microfluid. Nanofluid.* **2007**, *3*, 341–346.
31. Wang, W.; Ngan, K.H.; Gong, J.; Angeli, P. Observations on single drop formation from a capillary tube at low flow rates. *Colloids Surf. A Physicochem. Eng. Asp.* **2009**, *334*, 197–202.
32. Sugiura, S.; Nakajima, M.; Iwamoto, S.; Seki, M. Interfacial tension driven monodispersed droplet formation from microfabricated channel array. *Langmuir* **2001**, *17*, 5562–5566.
33. Thorsen, T.; Roberts, R.W.; Arnold, F.H.; Quake, S.R. Dynamic pattern formation in a vesicle-generating microfluidic device. *Phys. Rev. Lett.* **2001**, *86*, 18, 4163-4166.
34. Scheele, G.F.; Meister, B.J. Drop formation at low velocities in liquid-liquid systems: Part I. Prediction of drop volume. *AIChE J.* **1968**, *14*, 9–15. doi:10.1002/aic.690140105.
35. Leong, J.; Lim, T.; Pogaku, R.; Chan, E. Size prediction of k-carrageenan droplets formed in co-flowing immiscible liquid. *Particuology* **2011**, *9*, 637–643.
36. Umbanhowar, P.B.; Prasad, V.; Weitz, D.A. Monodispersed emulsion generation via drop break off in a coflowing stream. *Langmuir* **2000**, *16*, 347–351.
37. Baroud, C.N.; Gallaire, F.; Dangla, R. Dynamics of microfluidic droplets. *Lab Chip* **2010**, *10*, 2032–2045.
38. Chen, C.T.; Maa, J.R.; Yang, Y.; Chang, C. Drop formation from flat tip nozzles in liquid-liquid system. *Int. Commun. Heat Mass Transf.* **2001**, *28*, 681–692.
39. Schneider, T.; Chapman, G.H.; Hafeli, U.O. Effects of chemical and physical parameters in the generation of microspheres by hydrodynamic flow focusing. *Colloid Surf. B Biointerfaces* **2011**, *87*, 361–368.

40. Zhu, K.J.; Jiang, H.L.; Du, X.Y.; Wang, J.; Xu, W.X.; Liu, S.F. Preparation and characterization of hCG-loaded polylactide or poly(lactide-co-glycolide) microspheres using a modified water-in-oil-in-water (w/o/w) emulsion solvent evaporation technique. *J. Microencapsul.* **2001**, *18*, 247–260.
41. Gupta, A.; Matharoo, H.S.; Makkar, D.; Kumar, R. Droplet formation via squeezing mechanism in a microfluidic flow-focusing device. *Comput. Fluids* **2014**, *100*, 218–226.
42. Christopher, G.F.; Anna, S.L. Microfluidic methods for generating continuous droplet streams. *J. Phys. D Appl. Phys.* **2007**, *40*, R319–R336.
43. Nunes, J.K.; Tsai, S.S.H.; Wan, J.; Stone, H.A. Dripping and jetting in microfluidic multiphase flows applied to particle and fibre synthesis. *J. Phys. D Appl. Phys.* **2013**, *46*, 114002.
44. Tan, Y.; Cristini, V.; Lee, A.P. Monodispersed microfluidic droplet generation by shear focusing microfluidic device. *Sens. Actuators B* **2006**, *114*, 350–356.

Chapter 4

General Conclusions

Convective heat transfer inside a rectangular cavity can be influenced by position of partially active wall, presence of magnetic fields, and utilization of functional particles. Position of heat source along the vertical wall and the heat source facing direction on the horizontal axis as well as its intensity could affect performance of convective heat transfer inside the cavity. Direction, continuity, and intensity of applied magnetic field also have significant effects on the convective heat transfer performance. The utilization of functional particles also can support natural convection of heat transfer inside thermally-stratified fluid region of the rectangular cavity.

Regarding process of fabricating the spherical thermosensitive gels, size of the gel droplets can be adjusted by controlling the continuous-phase flow rate (silicone oil) and its kinematic viscosity. After polymerization of the gel droplets, shrinking and swelling behavior of the gels mostly influenced by temperature changes of the surrounding fluid which exhibited a negative thermal expansion. Based on the results, the gels required a certain length of time to thoroughly response to the temperature changes of the surrounding medium. Repetitive vertical motion of the thermosensitive gels inside the polymeric solution is mostly determined by buoyance force, gravity force, and drag force of the thermosensitive gels relative to their surrounding fluid. The time required for the gels to maintain their repetitive movements inside the polymeric solution is varied depending on their diametrical size. The gels with larger diameters tended to have longer vertical periodic movements and required more time to reach their equilibrium state compared to gels with smaller diameter.

Chapter 5

Future Study

Future study is recommended to improve swelling and shrinking behavior of the thermo-sensitive gels inside the polymeric aqueous solution inside the upper heating system of the rectangular cavity which are including:

a. Formulate new composition of the gels which having higher crosslinking density by increasing the mass amount of BIS (Methylene Bisacrylamide). The BIS can affect cross linker components of the gels and improve their swelling and shrinking behavior.
b. Create bigger size gels having diameter of 4 mm or more. By applying bigger size gels, longer time of the equilibrium state of the gels inside the system can be achieved. In accordance, effective number of the gels inserted inside the system should be found.
c. Create additional material as layers (shell or cover) on the surface of the gels which have hydrophobic characteristics that improve shrinking-swelling behaviors.

Acknowledgements

I would like to deliver my deep gratitude to ALLAH SWT as my God and Sustainer. Special thankful to Kanazawa University, especially for the School of Mechanical Science & Engineering in the Division of Natural Science and Technology as my lovely place of study to pursue my doctoral degree. I also would like to thank to Professor Dr. Eng. Yukio TADA as the Chief/Head Supervisor who always supervised and encouraged me to improve my work & research activities and Professor Nobuyoshi Kawabata as the former supervisor during my doctoral study. In addition, I would like to thank to Assistant Professor Dr. Eng. Masato Hasegawa who always give me assistance to improve my research activities and help me for the completion of my article publications. Moreover, I would like to thank to Associate Professor Masashi Haruki and Assistant Professor Hajime Onishi who supported me in Laboratory meetings. Thank also to Professor Satoshi Kitayama for the academic and social life counseling support in every year of my study. Thank also to Professor Akio Kodama and Associate Professor Yoshikazu Teraoka for academic teaching & support during my doctoral study. Thank also to my Laboratory team members: Kazuya Yamamoto, Kousuke Nakashima, Yu Norimatsu, and Ikuho Kurihara who always help me and has become my friends in the laboratory and my social life.

I also gratefully acknowledge to The Ministry of Research, Technology and Higher Education of Republic of Indonesia which later changed its name to Ministry of Education and Culture of Republic of Indonesia. Thanks to Halu Oleo University which provided me with administrative supports during the study. Thankful is also given to the bilateral cooperation between Kanazawa University and Directorate General of Resources for Science, Technology and Higher Education of the Ministry of Education

and Culture (KU-DIKTI Program). Special thankful is also given to Ministry of Finance of Indonesian Republic and Indonesia Endowment Fund for Education (LPDP) that give me a doctoral scholarship through BUDI-LN scheme and its continuity funding such as living allowance, family allowance and book allowance.

Great thankful also appreciate to Government of Japan that provides us a peace and lovely country to study and live in during the years. Kanazawa city is a beautiful and comfort place to stay in the Ishikawa Prefectures of Japan. I will not forget this country in the rest of my live.

Thankful is also given to the support of my family members: Nur Khoiriyyah (wife), Nurul Azizah, Shofiyyah An Nadzifah, and Najwa Salsabila Sisworo (children) who always stay with me and provide a spirit to finish my study in Kanazawa University, Japan.

Finally, I would like to underline that it is not easy to live lately in this situation during months when the deadly new-coronavirus disease is spreading to every part of the world and I have to finish my final steps in doctoral course while the disease is still threatening to my family members and affecting life of billions of humans in the world. Great appreciation is also attributed to Kanazawa University that provides excellent policies in combating the spreading of the new coronavirus in this campus.